THE ASTROPHYSICAL JOURNAL, 531:415–437, 2000 March 1

PHOTOMETRIC AND Ca II H AND K SPECTROSCOPIC VARIATIONS IN NEARBY SUN-LIKE STARS WITH PLANETS. III.[1]

GREGORY W. HENRY,[2] SALLIE L. BALIUNAS,[2,3,4] ROBERT A. DONAHUE,[3,4] FRANCIS C. FEKEL,[2,5] AND WILLIE SOON[3,4]
Received 1999 September 1; accepted 1999 October 15

ABSTRACT

We present the results of an analysis of time-series photometry, Ca II H and K spectrophotometry, and high-dispersion visible spectra of nine nearby Sun-like stars recently identified as having planets. For the six stars whose presumed planets have orbital periods of less than 4 months (τ Boo, 51 Peg, υ And, ρ^1 Cnc, ρ CrB, and 70 Vir), sine-curve fits to the photometric data show no variations with semi-amplitude greater than 1 or 2 parts in 10^4. Photometric variations in 47 UMa are similarly small, although our photometric data of this star are slightly affected by variability of the comparison star. Nonvariability at this level of precision is sufficient to rule out surface magnetic activity as the cause of the observed radial-velocity variations in these seven stars and makes nonradial pulsations unlikely as well. Thus, our photometry provides indirect but strong support for true reflex motions—planets—in these seven stars, but cannot yet so support the planetary hypothesis for the two additional stars, 16 Cyg B and Gl 411. Continued photometric monitoring of the short-period systems may soon result in the *direct* detection of these planets in reflected light. We have used our photometric fluxes to search for possible transits of the extrasolar planets. Transits definitely do not occur in τ Boo, 51 Peg, υ And, and ρ^1 Cnc, and probably do not occur in ρ CrB and 70 Vir. Our transit-search results are inconclusive for 47 UMa, and we cannot address the issue for 16 Cyg B and Gl 411. The precision of our photometry is sufficient to detect transits of planets even if they are not gas giants, as currently assumed, but much smaller objects with rocky compositions. The chance of finding at least one transit in the six stars is $\sim$40%. We find significant year-to-year photometric variability only in τ Boo, which is not only the youngest star in the sample but also the star with the shallowest convective zone. The interseasonal range in its yearly mean photometric flux is $\sim$0.002 mag, roughly twice the 0.0008 mag decadal variation in the Sun's total irradiance. Monitoring of the relative Ca II H and K fluxes began between 1966 and 1968 for 51 Peg, τ Boo, ρ CrB, and Gl 411, between 1990 and 1993 for 47 UMa, 70 Vir, 16 Cyg B, and ρ^1 Cnc, and in 1996 for υ And. The data have been newly recalibrated for improved long-term instrumental stability, resulting in better precision of the Ca II records. Five of the nine stars in this study have little or no detectable year-to-year variation in Ca II flux. The remaining four show moderate or pronounced variability: τ Boo, whose radial-velocity and photometric variations have comparatively high amplitudes; Gl 411, whose planetary companion was inferred astrometrically, not spectroscopically; ρ^1 Cnc, which may undergo decadal cyclic activity; and υ And, which shows moderate year-to-year variability. Except for 47 UMa, intraseasonal variability consistent with rotation was detected in the Ca II records of all stars. However, the rotation periods determined for υ And, 70 Vir, and 16 Cyg B are of low confidence. An examination of the recalibrated Ca II records for 51 Peg finds a rotation period of 22 days, in contrast to our previous result of 37 days. Ages have been estimated from the mean Ca II flux and, where possible, the rotation period. We find general consistency with the ages determined by others comparing properties determined from high-resolution spectroscopy to evolutionary models, although the uncertainties are, in general, large.

Subject headings: planetary systems — stars: activity — stars: late-type — techniques: photometric — techniques: spectroscopic

1. INTRODUCTION

At the Ninth Cool Stars Workshop in 1995 October in Florence, Italy, Mayor & Queloz (1996) reported evidence for an extrasolar planet in orbit around a lower main-sequence star (51 Peg). In the next 2 yr, eight additional solar-type stars were announced to have planetary-mass companions. We have previously analyzed photometric and Ca II H (396.8 nm) and K (393.3 nm) spectroscopic measurements of six of these stars (plus HD 114762, reported earlier to have a probable brown dwarf companion) to study photometric variability, surface magnetic activity, rotation, and age. Results for 51 Peg, 47 UMa, 70 Vir, and HD

[1] Based on observations made at Mount Wilson Observatory, operated by the Mount Wilson Institute, under an agreement with the Carnegie Institution of Washington and the automatic photoelectric telescope at Fairborn Observatory in the Patagonia Mountains of southern Arizona.

[2] Center of Excellence in Information Systems, Tennessee State University, 330 10th Avenue N., Nashville, TN 37203; henry@schwab.tsuniv.edu, baliunas@cfa.harvard.edu, fekel@coe.tnstate.edu.

[3] Harvard-Smithsonian Center for Astrophysics, 60 Garden Street, Cambridge, MA 02138; donahue@cfa.harvard.edu, wsoon@cfa.harvard.edu.

[4] Mount Wilson Observatory, 740 Holladay Road, Pasadena, CA 91106.

[5] Visiting Astronomer, Kitt Peak National Observatory, National Optical Astronomy Observatories, which is operated by the Association of Universities for Research in Astronomy (AURA), Inc., under cooperative agreement with the National Science Foundation.

114762 were discussed in Henry et al. (1997a, hereafter Paper I). Results for ρ^1 Cnc, τ Boo, and υ And were presented by Baliunas et al. (1997, hereafter Paper II). In this paper we discuss results on ρ CrB, 16 Cyg B, and Gl 411 (= Lalande 21185). We also provide new observations and analyses of the stars in Papers I and II and extend our search for photometric transits of the planets. Additional planetary candidates from new and extended planetary-search surveys continue to be announced (e.g., Mayor et al. 1998; Butler et al. 1998, 1999; Fischer et al. 1999); our observations and analyses of these additional stars and planets will be discussed in future papers.

Photometric and spectroscopic observations are an important component of current planetary-search programs, especially those based on radial-velocity techniques. Detailed knowledge of a star's surface magnetic activity and level of photometric variability can strengthen the inference of planetary companions based on radial-velocity observations alone. Variability in lower main-sequence stars, caused by, e.g., starspots, plages, or pulsations, may produce radial-velocity variations that are similar in amplitude and timescale to true reflex velocities (Hatzes 1996; Saar & Donahue 1997; Saar, Butler, & Marcy 1998). For example, periodic radial-velocity variations in HD 166435 were first attributed to planetary reflex motions, but were later found, from photometric and spectroscopic observations, to be caused by surface magnetic activity (Queloz et al. 1999). Thus, photometric and Ca II H and K observations can be used to explore alternative explanations for radial-velocity variations and so support or refute the inference of new planetary candidates. Moreover, the detection of a photometric transit of an extrasolar planet at the epoch of inferior conjunction would prove the existence of a planet and would lead directly to information concerning its true (as opposed to minimum) mass, size, and density. Those parameters are important for improving theoretical models of the composition and origin of extrasolar planets (e.g., Saumon et al. 1996; Guillot et al. 1997; Ward 1997; Boss 1997, 1998; Trilling et al. 1998; Sandquist et al. 1998; Marley et al. 1999; Seager, Whitney, & Sasselov 1999).

We describe our photometric, spectrophotometric, and spectroscopic observations in § 2 and detail the analyses of these data in § 3. The results for individual stars are discussed in § 4, and a general discussion of our findings is provided in § 5.

2. OBSERVATIONS

2.1. *Photometry*

Photometric observations were made with three automatic photoelectric telescopes (APTs) at Fairborn Observatory. Until 1996 July, Fairborn was located at the Fred L. Whipple Observatory on Mount Hopkins. During the summer of 1996, the APTs were relocated to Fairborn Observatory's new site at 5700 ft. in the Patagonia Mountains of southern Arizona (Eaton, Boyd, & Henry 1996).

The Vanderbilt–Tennessee State 0.4 m APT uses a temperature-stabilized EMI 9924B bi-alkali photomultiplier tube to acquire data through Johnson *B* and *V* filters. Each program star is measured in the following sequence, termed a group observation: K, sky, C, V, C, V, C, V, C, sky, K, where K is a check star, C is the comparison star, and V is the program star. Three V − C and two K − C differential magnitudes are calculated and averaged together to create group means. The group means are corrected for differential extinction with nightly extinction coefficients, transformed to the Johnson system with yearly mean transformation coefficients, and treated as single observations thereafter. External precision of the group means, based on standard deviations for pairs of constant stars, is 0.003–0.004 mag on good nights. This is roughly the scintillation noise expected in these observations.

The Smithsonian–Tennessee State 0.75 m APT and the Tennessee State–Smithsonian 0.80 m APT both use Strömgren *b* and *y* filters to make group observations in the sequence A, B, C, D, A, sky_A, B, sky_B, C, sky_C, D, sky_D, A, B, C, D, where A, B, and C are comparison stars, and D is the program star. The 0.75 m APT uses a single, temperature-stabilized EMI 9124QB bi-alkali photomultiplier tube to make the *b* and *y* observations sequentially. The 0.80 m APT has a two-channel photometer that uses a dichroic filter to separate the Strömgren *b* and *y* passbands so that two EMI 9124QB phototubes can measure the bands simultaneously. This allows integration times on the 0.80 m APT to be longer (40 s) than on the 0.75 m APT (20–30 s) without decreasing the throughput of the observing program. Observations are reduced differentially with each of the comparison stars, corrected for atmospheric extinction with nightly extinction coefficients, transformed to the Strömgren system, and combined into group mean differential magnitudes, which are then treated as single observations. Finally, we combine the *b* and *y* filter data, $(b + y)/2$, to increase precision, as done by Lockwood, Skiff, & Radick (1997) in their manual photometry of solar-type stars. External precision of single observations from the 0.75 m APT averages about 0.0015 mag on good nights; precision of the 0.80 m APT is about 0.0011 mag. As is the case for the measurements made by the 0.4 m APT, scintillation noise is the dominant source of error for the measurements made by the larger APTs.

All three telescopes make extensive observations of standard stars each night to allow us to determine the nightly extinction and to track any long-term instrumental changes. Since the APTs collect data whenever they can find stars, they sometimes do so under less than optimal conditions. Therefore, we use the standard deviation of the group mean magnitudes (a measure of the internal precision) and the quality of the standard-star solutions to discard poor measurements. Further details of telescope operations and data-reduction procedures can be found in Paper I and Henry (1995a, 1995b, 1999).

2.2. Ca II *H and K Spectrophotometry*

The Ca II H and K measurements were made with the 100 inch (1966–1977 and 1995–present) and 60 inch (1978–1995) telescopes at Mount Wilson Observatory as part of the ongoing HK Project (Baliunas et al. 1998). In that program, measurements of the Ca II H and K lines for several thousand stars are made as a proxy for surface magnetism.

The observed quantity, *S*, is the flux measured in two 0.1 nm passbands centered on the H and K lines normalized by two 2.0 nm wide sections of photospheric flux centered at 390.1 and 400.1 nm. A nightly calibration factor is determined from measurements of a standard lamp and standard stars (Baliunas et al. 1995). The night-to-night rms precision of the lamp is on the order of 0.5%, while the standard stars have an average standard deviation of ∼1.5%, which limits the lowest amplitude of variability that can be detected on timescales of years to approximately 1%.

In his survey of stellar activity cycles, Wilson (1978) used 18 standard stars. Over the course of continued monitoring, several of these stars have been dropped as standard stars because they began to show significant low-amplitude variations over decades. To improve the precision of the stellar records, we have replaced the most variable standard stars with stars of spectral classes A0–F0, under the assumption that their Ca II flux variations should be nearly, if not completely, absent.

In the last 2 yr we have not only incorporated the new standard stars, but also revised our data-calibration procedure. We have recalibrated and reanalyzed all of the Ca II records for the stars presented here. In most cases, the rotation periods inferred from the records with the new calibration are similar to the previously published values. For some stars, new detections of low-amplitude rotational modulation have been made, which, in turn, have led us to review some of the results presented in Papers I and II.

2.3. *Spectroscopy*

High-dispersion spectroscopic observations were obtained at the Kitt Peak National Observatory (KPNO) with the coudé feed telescope, coudé spectrograph, and a TI CCD. The wavelength region observed was centered at 643.0 nm. The spectra have a wavelength range of 8.0 nm, an instrumental resolution of 0.021 nm, corresponding to a velocity resolution of 9.8 km s^{-1}, and a typical signal-to-noise ratio of 200 or more.

With the procedure of Fekel (1997), rotational velocities were determined from the KPNO red-wavelength spectra for all stars except υ And. The FWHM of about a half-dozen weak or moderate-strength lines was measured and the results averaged. Instrumental broadening was removed, and the calibration polynomial of Fekel (1997) was used to convert the resulting broadening in nm into a total line broadening in km s^{-1}. For Gl 411 and ρ^1 Cnc, a macroturbulence of 2 km s^{-1} was assumed, while for τ Boo, 4 km s^{-1} was used. For all other stars, the assumed value was 3 km s^{-1}. The errors estimated for the rotational velocities range from 0.5 to 1.5 km s^{-1} and depend on the value of the rotational velocity itself and the number of spectra obtained. Uncertainties are greatest for the stars having the smallest $v \sin i$ values, since their line widths are dominated by macroturbulence rather than rotation. The number of spectra range from a single one for both Gl 411 and 51 Peg to eight for τ Boo. Four of the stars appear in the compilation of Fekel (1997), and for two, 70 Vir and ρ^1 Cnc, no additional observations have been obtained. However, the number of observations for τ Boo has increased from six to eight, while the number for 16 Cyg B has gone from one to four. Our new $v \sin i$ values for those stars supersede the values of Fekel (1997); values for the other four stars are new results.

3. ANALYSES

Tables 1 through 6 summarize the stellar and planetary properties of the nine systems and the results of our analyses. All tables list the stars in order of increasing orbital period of the planetary companions.

Table 1 gives stellar properties. Distances are derived from parallaxes in the *Hipparcos* catalogue (Perryman et al. 1997). Except where noted, metallicities and masses are from Gonzalez (1997, 1998) and Gonzalez & Vanture (1998). The sources of the effective temperatures (T_{eff}) are discussed individually below, along with other quantities used to compute absolute magnitudes, luminosities, and radii.

Table 2 summarizes properties of the extrasolar planets and their orbits, including orbital period, eccentricity, orbital radius, radial-velocity amplitude, mass, and the citation for the discovery of each object. When available, updated values obtained through private communications are listed.

Table 3 summarizes our precision photometry on each star. The yearly mean magnitudes are in the Strömgren $(b + y)/2$ bandpass, except for Gl 411, which is in the Johnson $(B + V)/2$ bands. The standard deviations (σ) are the deviations of single observations from the yearly mean magnitudes and are measures of the night-to-night variability in each star. All values of σ are near the expected limits of precision for their respective instruments, which implies that measurable short-term variability is not present in any star. Also listed are the standard deviations of the mean magnitudes (σ_{mean}), i.e., the standard deviation (col. [6]) divided by the square root of the number of observations for the year (col. [4]). These are typically 0.0001 or 0.0002 mag and demonstrate the precision with which we measure the yearly means.

Table 4 gives the results of our photometric analyses. The semiamplitudes are derived from sine-curve fits to the photometric data, assuming the planetary orbital periods given in Table 2, and serve as estimates of the maximum

TABLE 1

PROPERTIES OF SUN-LIKE STARS WITH PLANETS

HD Number	Name	Spectral Type	Distance (pc)	[Fe/H]	$M/M_\odot$	T_{eff} (K)	M_v	$L/L_\odot$	$R/R_\odot$
120136	τ Boo	F7 V	15.6	+0.34	1.36	6450	3.53	3.08	1.41
217014	51 Peg	G2–3 V	15.4	+0.21	1.05	5793	4.54	1.33	1.15
9826	υ And	F8 V	13.5	+0.17	1.31	6212	3.44	3.44	1.60
75732	ρ^1 Cnc	G8 V	12.5	+0.45	1:	5250	5.46	0.63	0.96
143761	ρ CrB	G0–2 V	17.4	−0.29	0.96	5777	4.20	1.77	1.31
117176	70 Vir	G4 V–IV	18.1	−0.03	1.10	5488	3.68	3.02	1.93
186427	16 Cyg B	G2.5 V	21.4	+0.06	0.97	5760	4.56	1.31	1.15
95128	47 UMa	G0 V	14.1	+0.01	1.03	5882	4.30	1.60	1.22
95735	Gl 411	M2 V	2.55	−0.20[a]	0.42[b]	3350	10.47	0.02	0.37

[a] From Mould 1978.
[b] Estimated mass for M2 V.

TABLE 2

PROPERTIES OF EXTRASOLAR PLANETS

Planet	P_{orb} (days)	Eccentricity	Orbital Radius (AU)	RV Amplitude (m s^{-1})	Mass (M_{Jup})	Discoverer
τ Boo b	3.31275	0.0	0.046	463	≥3.39	1
51 Peg b	4.2310	0.0	0.051	56.0	≥0.45	2
υ And b	4.6170	0.03	0.059	73	≥0.71	1
ρ^1 Cnc b	14.649	0.0	0.11	76.4	≥0.91	1
ρ CrB b	39.90	0.13	0.23	67	≥1.1	3
70 Vir b	116.67	0.405	0.43	318	≥6.98	4
υ And c	241	0.2	0.83	58	≥2.11	5
16 Cyg B b	857	0.68	1.6	54	≥1.83	6
47 UMa b	1035	0.07	2.1	46	≥2.28	7
υ And d	1267	0.4	2.5	73	≥4.61	5
Gl 411 b	2100	0.0	2.2	<190[a]	~0.9	8

[a] Measure of velocity rms from Marcy & Benitz 1989.

REFERENCES.—(1) Butler et al. 1997; (2) Mayor & Queloz 1995; (3) Noyes et al. 1997a, 1997b; (4) Marcy & Butler 1996; (5) Butler et al. 1999; (6) Cochran et al. 1997; (7) Butler & Marcy 1996; (8) Gatewood 1996.

photometric variability possible at the orbital period. Because the orbital periods obtained from the radial-velocity data have been determined to high precision (i.e., ≪0.1%), our assessment of photometric semiamplitude is not significantly altered if we permit the period of the sine curve to vary within several standard deviations of the period measurement error. All semiamplitudes in Table 4 are within 1–2 σ of zero; i.e., within the uncertainties of the photometry, the stars are constant at the orbital periods. A measure of the long-term (year-to-year) variability of each star, σ_{long}, is given as the standard deviation of the star's yearly mean magnitudes (from col. [5] of Table 3) with

TABLE 3

SUMMARY OF PHOTOMETRIC OBSERVATIONS

Star (1)	APT (2)	Date Range (JD − 2,400,000) (3)	N_{obs} (4)	Yearly Mean (mag) (5)	σ (mag) (6)	σ_{mean} (mag) (7)
τ Boo	0.75	49094–49164	43	−1.6957	0.0015	0.0002
		49345–49547	63	−1.6954	0.0015	0.0002
		49725–49890	58	−1.6970	0.0015	0.0002
		50085–50241	51	−1.6960	0.0013	0.0002
		50436–50635	234	−1.6949	0.0017	0.0001
		50795–50993	63	−1.6967	0.0016	0.0002
51 Peg	0.75	49145–49362	51	−0.6471	0.0011	0.0002
		49512–49666	30	−0.6474	0.0012	0.0002
		49879–50091	57	−0.6477	0.0009	0.0001
		50265–50458	24	−0.6473	0.0015	0.0003
		50714–50828	34	−0.6473	0.0017	0.0003
υ And	0.80	50392–50494	33	−1.8783	0.0010	0.0002
		50718–50867	88	−1.8781	0.0010	0.0001
ρ^1 Cnc	0.80	50394–50573	58	−0.1922	0.0015	0.0002
		50726–50960	152	−0.1922	0.0013	0.0001
ρ CrB	0.75	49094–49163	43	−0.3079	0.0009	0.0001
		49372–49547	56	−0.3076	0.0010	0.0001
		49750–49892	60	−0.3077	0.0011	0.0001
		50109–50265	48	−0.3077	0.0012	0.0002
		50466–50631	60	−0.3090	0.0013	0.0002
		50823–50995	137	−0.3086	0.0017	0.0001
70 Vir	0.75	49094–49164	44	−0.7852	0.0015	0.0002
		49339–49546	53	−0.7856	0.0011	0.0002
		49718–49908	67	−0.7864	0.0014	0.0002
		50071–50249	57	−0.7870	0.0013	0.0002
		50434–50635	73	−0.7862	0.0016	0.0002
		50795–50993	93	−0.7881	0.0019	0.0002
47 UMa	0.75	50037–50240	93	−1.1478	0.0014	0.0001
		50408–50618	58	−1.1487	0.0015	0.0002
		50768–50988	91	−1.1486	0.0015	0.0002
Gl 411	0.40	50432–50635	136	0.5747	0.0034	0.0003
		50741–50997	160	0.5749	0.0033	0.0003

TABLE 4

RESULTS OF PHOTOMETRIC ANALYSIS

Star	Semiamplitude (mag)	σ_{long} (mag)	Geometric Transit Probability	Transits
τ Boo..........	0.00011 ± 0.00009	0.0008	0.14	No
51 Peg.........	0.00021 ± 0.00013	0.0002	0.11	No
υ And	0.00016 ± 0.00013	0.0001	0.13	No
ρ^1 Cnc	0.00011 ± 0.00009	0.0000	0.041	No
ρ CrB	0.00011 ± 0.00009	0.0001[a]	0.026	No?
70 Vir	0.00020 ± 0.00011	≤0.0010[b]	0.021	No?
16 Cyg B......	...	...	0.0033	?
47 UMa.......	≤0.00048 ± 0.00013[c]	≤0.0004[c]	0.0027	?
Gl 411.........	...	0.0001	0.00078	?

[a] Excludes the mean magnitude from the fifth and sixth observing seasons for reasons cited in the text.
[b] Upper limit, because the K0 III comparison star is probably variable.
[c] Upper limit, because the K2 III comparison star is probably variable.

respect to the mean of the star's mean magnitudes. Most, but not all, are near the 0.0001–0.0002 mag limit of precision for yearly means, indicating no long-term variability at this level. The listed geometric probability that photometric transits of a planet can occur is computed as the ratio of the stellar radius to the semimajor axis of the planetary orbit (Schneider 1996). Finally, the results of our search for these photometric transits are given.

Table 5 summarizes the analysis for stellar axial rotation determined from the spectra and Ca II records. The values of $v \sin i$ found from spectra are from this work, except for υ And. Following the $v \sin i$ values in the table are the predicted rotation period, P_{calc}, which is based on a star's $B-V$ color index and the average Ca II flux, $\langle S \rangle$ (Noyes et al. 1984), and periods seen in the Ca II records. Those periods were determined from periodogram analysis (Horne & Baliunas 1986) for each observing season (~120–150 nights) that had sufficient observations (typically 30 or more observations on 10 or more nights). The mean period, $\langle P \rangle$, the rms and range of periods found, and the number of seasons, N_P, in which a period that might be attributable to rotational modulation was detected are also given in Table 5. A range of periods or secular changes in the observed period may be caused by surface differential rotation (Baliunas et al. 1985; Donahue 1993) or the influence of active-region growth and decay, or both, but detailed analysis of these effects is beyond the scope of this paper. We also assign a subjective grade for the quality of the period detection as confirmed, probable, or weak. The grade is based on two criteria: (1) whether a period occurs near the same frequency in more than one season; and (2) the significance of the periodogram peak(s).

Table 6 summarizes the year-to-year variability of the Ca II records on timescales of years. Four of the nine stars have been observed regularly since 1966, and their records are shown in Figure 1. The others were added subsequently as part of an extended program concentrating on a sample of stars with $B-V$ and $\langle S \rangle$ close to the Sun's, or after the detection of an extrasolar planet (in the case of υ And), and their records are shown in Figure 2. The average Ca II flux, $\langle S \rangle$, is calculated over the length of the entire record from the mean value of 30 day averages of S. This was done because the frequency of observations before and after 1980 is substantially different. Prior to 1980, a set of 4–5 obser-

TABLE 5

ANALYSIS FOR ROTATION

Star Name (1)	$v \sin i$ (km s^{-1}) (2)	P_{calc}[a] (days) (3)	$\langle P \rangle$ (days) (4)	rms (P)[b] (days) (5)	P range (days) (6)	N_P (7)	Grade[c] (8)
τ Boo..........	14.9 ± 0.5	5.1	3.2	0.5	2.6–4.1	13	Probable
51 Peg.........	1.3 ± 1.5	29.5	21.9	0.7	21.3–22.6	3	Weak
υ And	9.0 ± 0.4[d]	11.6	14	5	11–19	2	Weak
ρ^1 Cnc	2.2 ± 1	42.2	39	3	35–43	5	Confirmed
ρ CrB	2.1 ± 0.5	19.9	19	2	17–20	5	Confirmed
70 Vir	1.2 ± 1	35.8	31	3	29–34	3	Weak
16 Cyg B......	1.5 ± 1	27.4	31	9	25–38	2	Weak
47 UMa.......	2.0 ± 1	21.0[e]	74	...	...	1	Weak
Gl 411.........	1.4 ± 1.5	...[f]	56	3	52–60	6	Confirmed
			33	3	30–35	3	Probable

[a] Using the method of Noyes et al. 1984.
[b] The rms of the distribution of measurements of P about $\langle P \rangle$, and not the error in $\langle P \rangle$.
[c] Grade is a subjective estimate of the quality of the determination of rotation period.
[d] Gray 1986.
[e] Assuming that 47 UMa is on the main sequence.
[f] The formula for estimating P_{calc} based on $\langle S \rangle$ and $B-V$ by Noyes et al. 1984 is limited to stars with $B-V < 1.2$.

TABLE 6

LONG-TERM Ca II H AND K MONITORING

Name (1)	HD (2)	HR (3)	$B-V$ (4)	$\langle S \rangle$[a] (5)	$\sigma_S/\langle S \rangle$[b] (%) (6)	N_{30}[c] (7)	N_{total}[d] (8)	log R'_{HK} (9)	Age[e] (Gyr) (10)	Multiyear Variability (11)
τ Boo	120136	5185	0.48	0.1906	4.2	174	3562	−4.733	∼1	Variable
51 Peg	217014	8729	0.67	0.1500	3.0	130	2055	−5.068	3–7[f]	Long
υ And	9826	458	0.54	0.1611	4.7	20	216	−4.927	<4	Variable
ρ^1 Cnc	75732	3522	0.87	0.1900	6.4	37	384	−4.949	4–5	Cyclic?
ρ CrB	143761	5968	0.60	0.1498	1.4	176	3983	−5.048	6	Long
70 Vir	117176	5072	0.71	0.1445	4.6	42	556	−5.115	8	Long
16 Cyg B	186427	7504	0.66	0.1539	13.8	31	457	−5.039	6–7	Cyclic?
47 UMa	95128	4277	0.61	0.1514	2.8	39	557	−5.041	6[g]	Long/Low Amp.
Gl 411	95735	...	1.51	0.4215	10.9[h]	153	1684	...[i]	...	Variable?

[a] $\langle S \rangle$ is the mean value of 30 day means of S. It is calculated in this manner to account for differences in data sampling before and after 1980 (Baliunas et al. 1995).

[b] $\sigma(S)$ is the rms of the 30 day means.

[c] The number of 30 day means.

[d] The total number of observations. After 1979, three sequential observations were made per night when the star was observed.

[e] Listed determinations are from our analysis of the Ca II records; see text.

[f] Ages from $\langle S \rangle$ and $\langle P \rangle$ do not agree. See text.

[g] Assuming that 47 UMa is on the main sequence.

[h] Occasional flare activity inflates the values of $\langle S \rangle$ and $\sigma(S)$.

[i] The conversion from S to log R'_{HK} is inaccurate for stars with $B-V > 1.2$.

vations per month were usually made (near full moon). After 1980, 1–5 sets of three sequential observations were scheduled every week. Thus, a simple average of S over the interval 1966–present would weight the average toward the most recent data. In Table 6, N_{30} is the number of 30 day means used to calculate $\langle S \rangle$, and N_{total} is the total number of observations.

The ages listed in Table 6 were determined from the mean Ca II flux by means of a relationship between magnetic activity and age (Soderblom, Duncan, & Johnson 1991; Donahue 1998). An accurate determination of age from the mean measure of activity requires that the Ca II flux be averaged over effects such as rotation, growth and decay of Ca II–emitting regions, activity cycles, and longer period variations (e.g., Maunder minima). If only a few observations of the Ca II fluxes of a star such as the Sun at random phases of long-term activity fluctuations are available, then its age may have an uncertainty of ∼2–3 Gyr. For stars whose Ca II records are well sampled over several activity cycles (or the characteristic timescale of variability if it is not cyclic), the uncertainty in age determined from $\langle S \rangle$ is improved because the variations causing uncertainty have been more properly averaged. If a star is in an undetected Maunder minimum phase (which can last for several decades), the age can be overestimated by several (∼2–5) Gyr.

Donahue (1998) used a sample of $\gtrsim$20 binaries whose Ca II records ranged from as short as one night to as long as several decades to determine the distribution of uncertainty that would be introduced in an age estimate by activity variability, and found that for stars older than 2 Gyr, the age discrepancy is typically below 1 Gyr. This sets a rough indication of the uncertainty of activity-derived ages.

The age estimate may also be improved if the rotation period is known. However, as mention above, surface differential rotation is undoubtedly present, and consequently, the age estimated from one or only a few measurements of rotation period may be uncertain. For inactive stars with flat activity records, rotation is a better indicator of age than activity, since rotation can reveal whether a star is in a temporary Maunder minimum state—the rotation in that case is anomalously rapid for the average activity level. However, the likelihood of detecting rotational modulation during a Maunder minimum is smaller, because of lower activity.

Given the mass (e.g., $B-V$ color index) of a lower main-sequence star and one of three parameters (age, rotation period, or mean activity level), the other two parameters can be calculated. The parameters are coupled through a mechanism like the magnetic dynamo, but the explicit form of the coupling between parameters has only been determined empirically.

For the stars with long records or for which rotation has been well determined, our age estimates are fairly good, perhaps $\lesssim$1 Gyr. In the case of a star with a shorter (<20 yr) time series but well-determined rotation period, the age uncertainty may be on the order of ∼1 Gyr. If rotation has been detected (but not resolved over surface differential rotation), the age uncertainty is possibly ∼1–3 Gyr.

Planets orbiting active (i.e., younger and more rapidly rotating) stars should be harder to detect owing to the presence of surface inhomogeneities larger in area or covering more of the surface that introduce fluctuations in the precise radial-velocity measurements through changes in spectral line shapes (Saar & Donahue 1997). In some cases, changing line shapes may mimic radial-velocity variability and erroneously suggest a planet at the rotation period, for example HD 166435 (Queloz et al. 1999). Five of the stars in Table 6, 51 Peg, ρ CrB, 70 Vir, 16 Cyg B, and 47 UMa, are relatively inactive in Ca II fluxes, i.e., they show low average surface activity and little flux variability.

In terms of the pattern of variation in the Ca II H and K fluxes on timescales of decades, Baliunas et al. (1995) classified 51 Peg and Gl 411 as variable, (i.e., significant variability without pronounced periodicity), listed a small-amplitude cycle period of ∼12 yr for τ Boo, and classified ρ CrB as long (i.e., with a timescale longer than 25 yr). Classes in Table 6 differ because we now regard τ Boo as

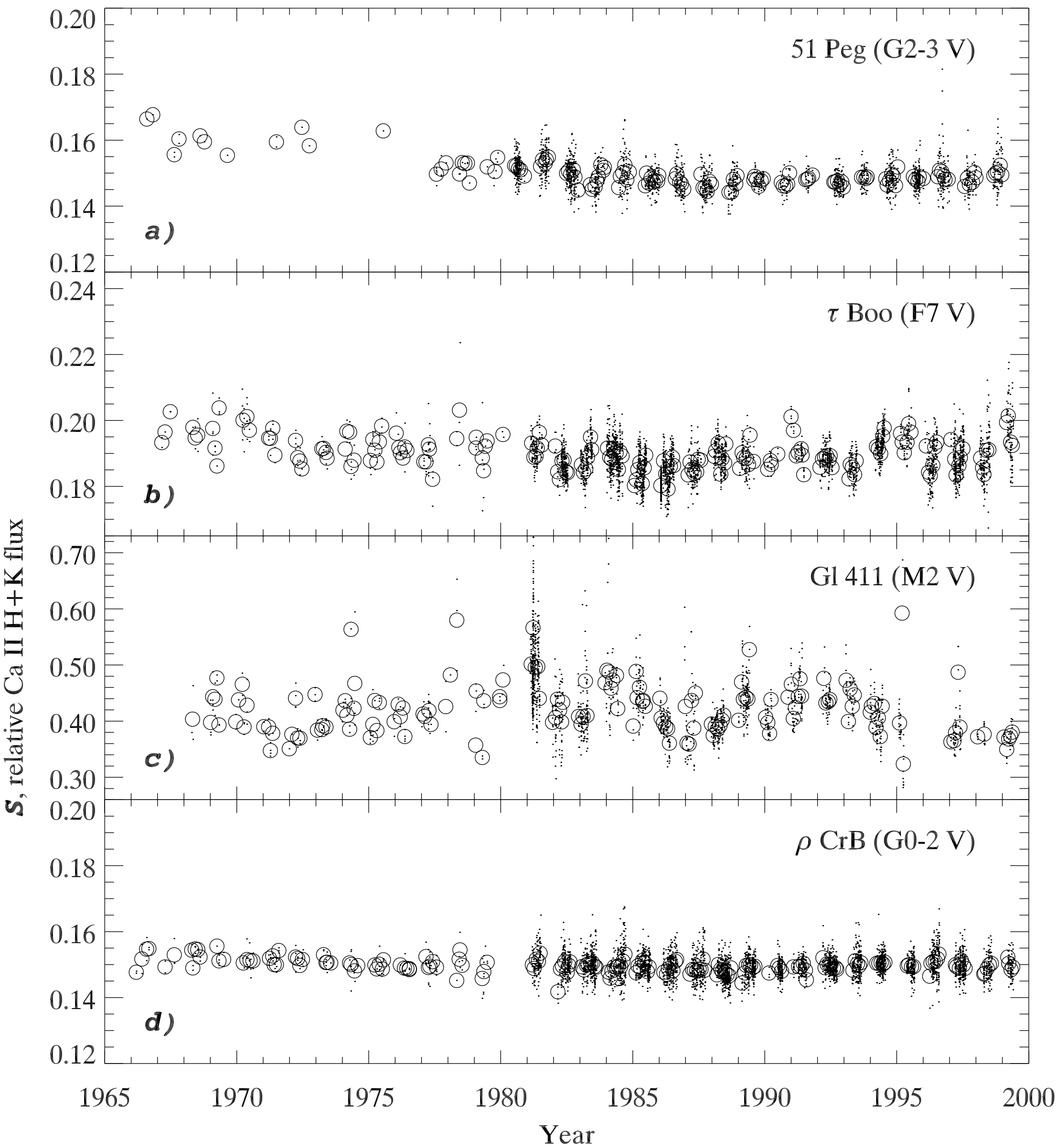

FIG. 1.—Long-term activity records of 51 Peg (HD 217014, G2-3 V), τ Boo (HD 120136, F7 V), Gl 411 (HD 95735, M2 V), and ρ CrB, (HD 143761, G0–2 V) are shown (*small dots*), overplotted with 30 day means (*open circles*).

variable and 51 Peg as long, as a result of the longer record and improved data calibration used here. Gl 411 is still classified as variable.

4. DISCUSSION OF INDIVIDUAL STARS

The nine stars are discussed below in the same order as they are listed in Tables 1–6 above, i.e., in order of increasing orbital period of their planetary companions. The mass and radius estimates used in these discussions to predict possible transit depths are based on the assumption that the planetary orbital inclinations are 90°, so that the true planetary masses would equal the minimum masses found from the radial-velocity observations.

4.1. *τ Boo (= HD 120136 = HR 5185)*

The companion to τ Boo was discovered by Butler et al. (1997). Stellar properties were discussed in that paper and in Paper II; these properties are summarized in Table 1. We have computed the absolute magnitude, luminosity, and radius in Table 1, with $V = 4.50$ and $B-V = 0.48$ from Mermilliod & Mermilliod (1994), $T_{\rm eff} = 6450$ K from Perrin et al. (1977), and a bolometric correction of -0.004 (Flower 1996). Properties of the planet and its orbit given in Table 2 are from Butler et al. (1997), with updates from G. W. Marcy (1998, private communication).

4.1.1. *Photometry*

After Gray (1997) announced that nonradial pulsations in 51 Peg might explain its observed radial-velocity variations (see discussion below), we planned extensive photometric and Ca II H and K spectroscopic observations of τ Boo during 1997. With a velocity amplitude nearly 10 times larger than that of 51 Peg, τ Boo might be expected to show photometric effects arising from pulsations if pulsations were the cause of the radial-velocity variations. In 1997 April, we acquired 234 group observations with the 0.75 m APT by devoting several nights around the time of opposition to constant monitoring of τ Boo and its comparison stars.

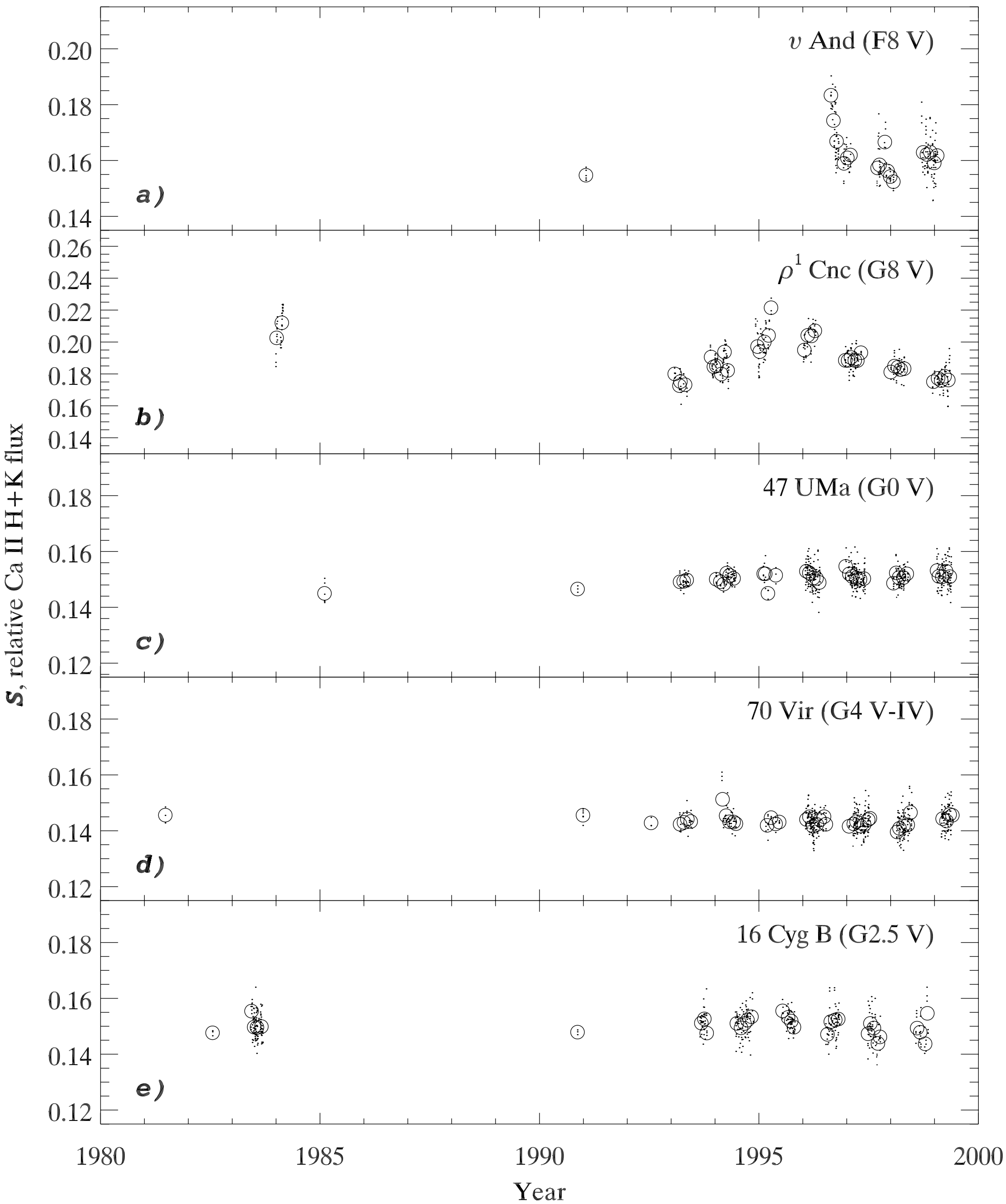

FIG. 2.—Long-term activity records of υ And, (HD 9826, F8 V), ρ^1 Cnc, (HD 75732, G8 V), 47 UMa, (HD 95128, G0 V), 70 Vir, (HD 117176, G4 V–IV), and 16 Cyg B, (HD 186427, G2.5 V) are shown (*small dots*), overplotted with 30 day means (*open circles*).

Our 6 yr of photometry, including the intensive monitoring in 1997, are summarized in Table 3. The yearly mean magnitudes are differential $(b + y)/2$ magnitudes, in the sense of τ Boo minus the comparison star HD 121560 (F6 V). It is apparent that τ Boo exhibits year-to-year brightness changes; the mean magnitudes vary by 0.002 mag, 10 times their mean errors. We see precisely the same variations when τ Boo is measured with respect to another comparison star (HD 120601, F0). There is a faint M dwarf companion ($\Delta m \sim 7$) located only 5″ from τ Boo that is included in the photometer diaphragm whenever we measure τ Boo. For this faint companion to account for the observed year-to-year variations in τ Boo, it would have to vary by a factor of 2, an unlikely scenario. Therefore, we can conclude that the observed variations are indeed intrinsic to τ Boo itself. The standard deviation of the yearly means from the mean of the means, the measure of long-term variability, is 0.0008 mag (Table 4), significantly larger than the precision with which we typically measure the yearly means.

To search for photometric pulsations at the value of the inferred orbital period of the planet, the year-to-year photometric variation was removed by shifting the data from each season to the mean brightness of the first observing season. The adjusted photometric flux is plotted in Figure 3 (*top*) against the orbital phase of the planetary companion com-

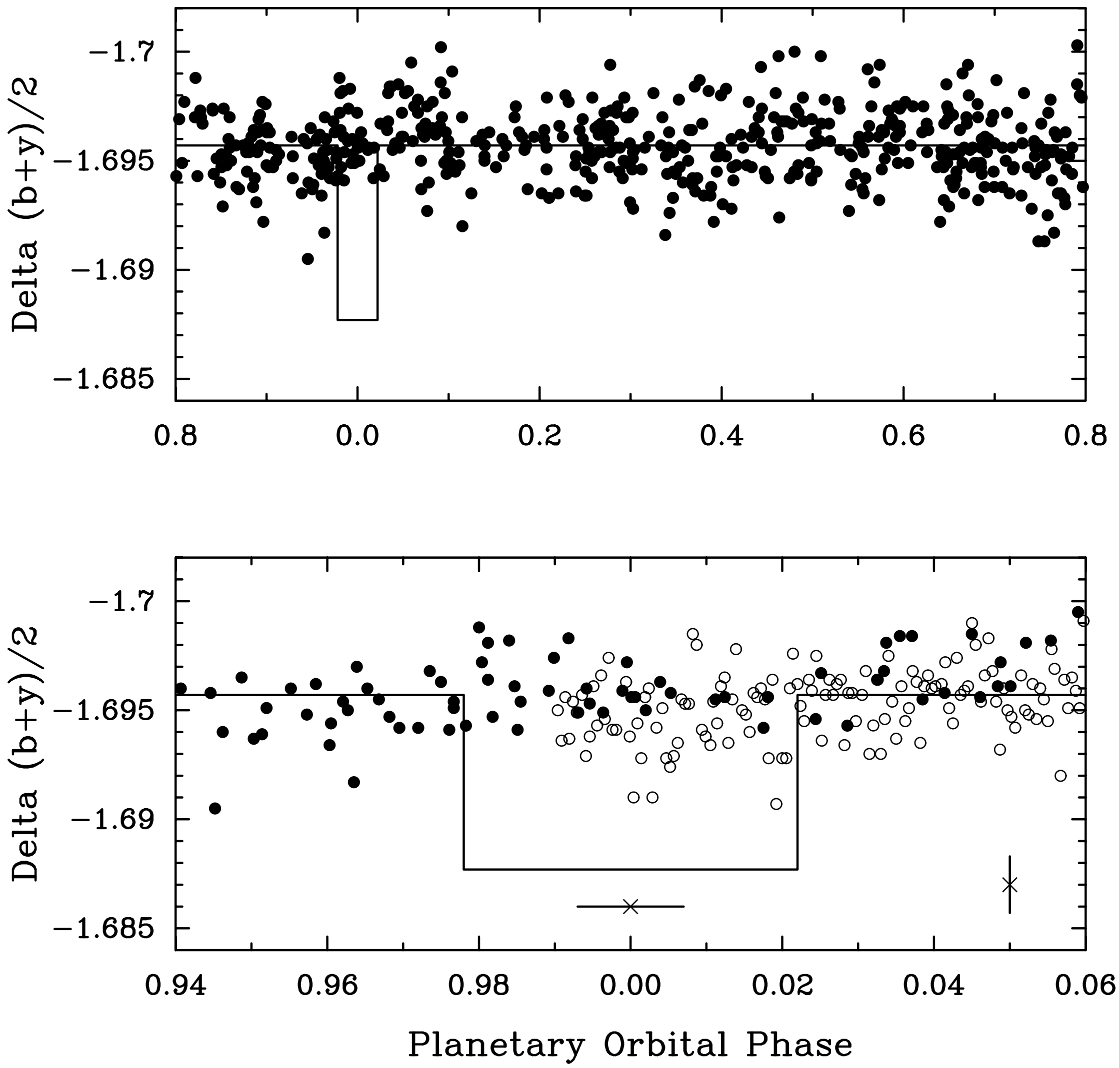

FIG. 3.—*Top*: Six seasons of nightly Strömgren $(b + y)/2$ differential magnitudes of τ Boo plotted modulo the 3.31275 day orbital period of the companion. Phase 0.0 corresponds to the time of conjunction when the companion would transit the star for suitable orbital inclinations. A least-squares sine fit at the orbital period yields a semiamplitude of 0.00011 ± 0.00009 mag. The solid line shows the predicted drop in light for the transit of a $1.2R_{\rm Jup}$ planet across the 1.41 $R_{\odot}$ star. *Bottom*: Photometric observations of τ Boo (*filled circles*) near the time of conjunction replotted with an expanded scale on the abscissa. An additional night of intensive observations with the 0.80 m APT from the 1997 observing season has been added (*open circles*; see text). Although the probability of transits is 14%, our photometric observations clearly show that they do not occur. The error bar in the lower right of the panel refers to the mean precision of a single observation. The error bar immediately below the transit window refers to the uncertainty in the predicted time of midtransit.

puted with the ephemeris

$$\mathrm{JD_{conj}} = 2{,}450{,}216.351 + 3.31275E \qquad (1)$$

of G. W. Marcy (1998, private communication). Zero phase is the time of midtransit for favorable orbital inclinations.

The semiamplitude of a sine-curve fit to the data with the period fixed to the planetary orbital period is 0.00011 ± 0.00009 mag (Table 4). This result is a tighter constraint on variability than we were able to report in Paper II. Periodogram analysis of the individual seasons and of the six seasons taken together reveal no significant periods, including the unexplained 116 day periodicity in the Ca II record reported in Paper II (see § 4.1.2). The small standard deviations of the nightly observations (Table 3, col. [6]) provide additional evidence for the short-term photometric nonvariability of τ Boo. These results, plus the lack of periodic changes in the shapes of τ Boo's spectroscopic line profiles (Brown et al. 1998; Hatzes & Cochran 1998), support the conclusion that a planet is the source of the radial-velocity variations.

The bottom panel of Figure 3 shows an expanded portion of the phase curve around the time of conjunction; an additional night of intensive observations from the 0.80 m APT scheduled within the predicted phases of a possible planetary transit has been added (*open circles*). These observations were not included in the sine-curve fitting (Fig. 3, *top*) to avoid biasing in the phase distribution. The solid line shows the drop in light that would result if τ Boo b were to transit centrally across the stellar disk. With a stellar radius of 1.41 $R_{\odot}$ and an orbital radius of 0.046 AU, transits could occur for orbital inclinations in the range $90° \pm 8\overset{\circ}{.}1$. The radius of the planet is computed to be $1.2R_{\rm Jup}$ by Guillot et al. (1997), so the photometric depth of a planetary transit would be 0.008 mag. The duration of a central transit would be ± 0.022 phase units, or 3.6 hr. The probability that τ Boo would show transits, among a group of stars with the same planetary system whose orbits are randomly inclined to the line of sight, is 14%. The uncertainty in the time of midtransit, according to G. W. Marcy (1998, private communication), is only about 36 minutes, or 0.007 phase units. It is clear from the figure that transits *do not* occur. The inclination of the orbit to our line of sight must be smaller than 82°.

4.1.2. Ca II *H and K Spectrophotometry*

τ Boo is the most massive as well as the youngest of our stars. The Ca II flux record for τ Boo is plotted in Figure 1. A $\sim$116 day period, reported in Paper II, appears in the Ca II fluxes, but not in the photometric or radial-velocity data. This variation is not explained by the familiar phenomena of rotation, growth and decay of surface features, or an activity cycle.

We find a rotation period of 3.2 days (Table 5), similar to but more confidently determined than the result in Paper II. We give a grade of probable to the mean value of 3.2 days, primarily because the amplitude of variation is weak. Despite the small amplitude, rotational modulation is seen in 13 seasons, with periods between $\sim$2.6 and 4.1 days, a range that may be an expression of surface differential rotation.

None of the observed periods approaches the predicted period of $P_{\rm calc} = 5.1$ days, which is calculated from $\langle S, 1966\text{–present}\rangle$. The $v \sin i = 14.9 \pm 0.5$ km s^{-1} is consistent with either the measured rotation period of 3.2 days or the estimated period, if the condition $v \sin i \leq v_{\rm max}$ is imposed, where $v_{\rm max}$ is the largest surface velocity (e.g., the equatorial velocity of the Sun), and assuming that the shortest period from the Ca II record is close to the equatorial periods.

The observed rotation period is similar to the planetary orbital period (3.3 days), and might indicate an influence of Ca II flux variability on radial-velocity variation and so seem to weaken the case for the existence of a planet. However, τ Boo has the largest radial-velocity amplitude of any of the stars in this sample (463 m s^{-1}), which is well in excess of the effects of surface magnetism and convection on velocity (Paper I). This is the only case in which the star's rotation period and the planet's orbital period of revolution are nearly equal.

The star's $\langle S\rangle$ and $B-V$ color imply an age of 2 Gyr: older, but not greatly so, than the estimates of 1.0 ± 0.6 Gyr (Fuhrmann, Pfeiffer, & Bernkopf 1998) and 1 ± 1 Gyr (Ford, Rasio, & Sills 1998). Gonzalez (1998) gives a younger age, less than 1 Gyr. Based on the star's observed rotation period of 3.2 days, we estimate an age of $\sim$1 Gyr, in agreement with the aggregate of ages estimated by other methods.

4.2. *51 Peg* (= *HD 217014* = *HR 8729*)

In Paper I, we analyzed 18 yr of Ca II H and K spectrophotometry and 2 yr of photometry of 51 Peg and found that the low surface magnetic activity and lack of photometric variability supported the existence of a short-period planet as the cause of the radial-velocity variations discovered by Mayor & Queloz (1995) and confirmed by Marcy et al. (1997). However, Gray (1997) announced the possible detection of spectroscopic line-profile variations that, if real, would refute the existence of a planetary companion in favor of nonradial pulsations in the star itself. Gray & Hatzes (1997) subsequently suggested pulsation modes that might be consistent with our nondetection of brightness variations (Paper I). However, further high-resolution spectroscopic observations during the 1997 observing season by Gray (1998), Hatzes, Cochran, Bakker (1998), and Brown et al. (1998) found no evidence of line-profile variations, so a low-mass companion remains the most plausible explanation for the radial-velocity variations. Our new photometry finds no significant photometric variability at the same level of nondetection as in Paper I (see below).

The properties of 51 Peg are discussed in Paper I, Mayor & Queloz (1995), Marcy et al. (1997), and Fuhrmann et al. (1997) and are summarized in our Table 1. The star is one of four stars found to be most like the Sun by participants of the Lowell Workshop on Solar Analogs (Hall 1998). We computed the absolute magnitude, luminosity, and radius in Table 1 with $V = 5.47$ and $B-V = 0.66$ from Mermilliod & Mermilliod (1994), $T_{\rm eff} = 5793$ K from Fuhrmann et al. (1997), and a bolometric correction of -0.098 (Flower 1996). Properties of the planet and its orbit from Mayor & Queloz (1995), Marcy et al. (1997), and updates from G. W. Marcy (1998, private communication) are given in Table 2.

4.2.1. *Photometry*

We have now acquired 196 high-quality nightly photometric observations over five observing seasons with the 0.75 m APT. The results are summarized in Table 3. The yearly mean magnitudes given in column (5) are differential $(b + y)/2$ magnitudes, in the sense of 51 Peg minus the comparison star HD 218235 (F6 V). The fifth yearly mean magnitude in Table 3 has been adjusted by 0.0026 mag because of an unexpected fading of HD 218235 by that amount, as confirmed with the other two comparison stars. The standard deviations of a single group observation from the yearly means have an average of 0.0013 mag, and so indicate no intraseason variability in 51 Peg. Periodogram analyses of the individual observing seasons and of the five seasons taken together reveal no significant periodicities between 1 and 100 days. The standard deviation of the yearly mean magnitudes (Table 3, col. [5]) from the mean of the mean magnitudes is 0.0002 mag (Table 4), indicating no detectable long-term variations in 51 Peg.

The photometric observations from the five observing seasons are plotted in the top panel of Figure 4 against the orbital phase of the planetary companion computed with the ephemeris

$$\mathrm{JD_{conj}} = 2{,}450{,}027.271 + 4.2310E \qquad (2)$$

of G. W. Marcy (1998, private communication). The individual observations in seasons 2–5 have been adjusted slightly, so that their yearly means equal the first yearly mean. A sine curve fitted to the adjusted data at the fixed planetary period has a semiamplitude of 0.00021 ± 0.00013 mag, essentially the same result that we obtained in Paper I.

The portion of the phase curve near the time of conjunction is replotted in the bottom panel of Figure 4, where two additional nights of intensive observations (not included in the top panel of Figure 4 for reasons explained in § 4.1.1) acquired with the 0.80 m APT have been added. The solid line shows the light curve that would result from a central transit of 51 Peg b. In this case, the geometry allows transits to occur for orbital inclinations in the range 90° ± 6°.0. The radius of the planet, assuming a mass of $0.45 M_{\rm Jup}$, should be

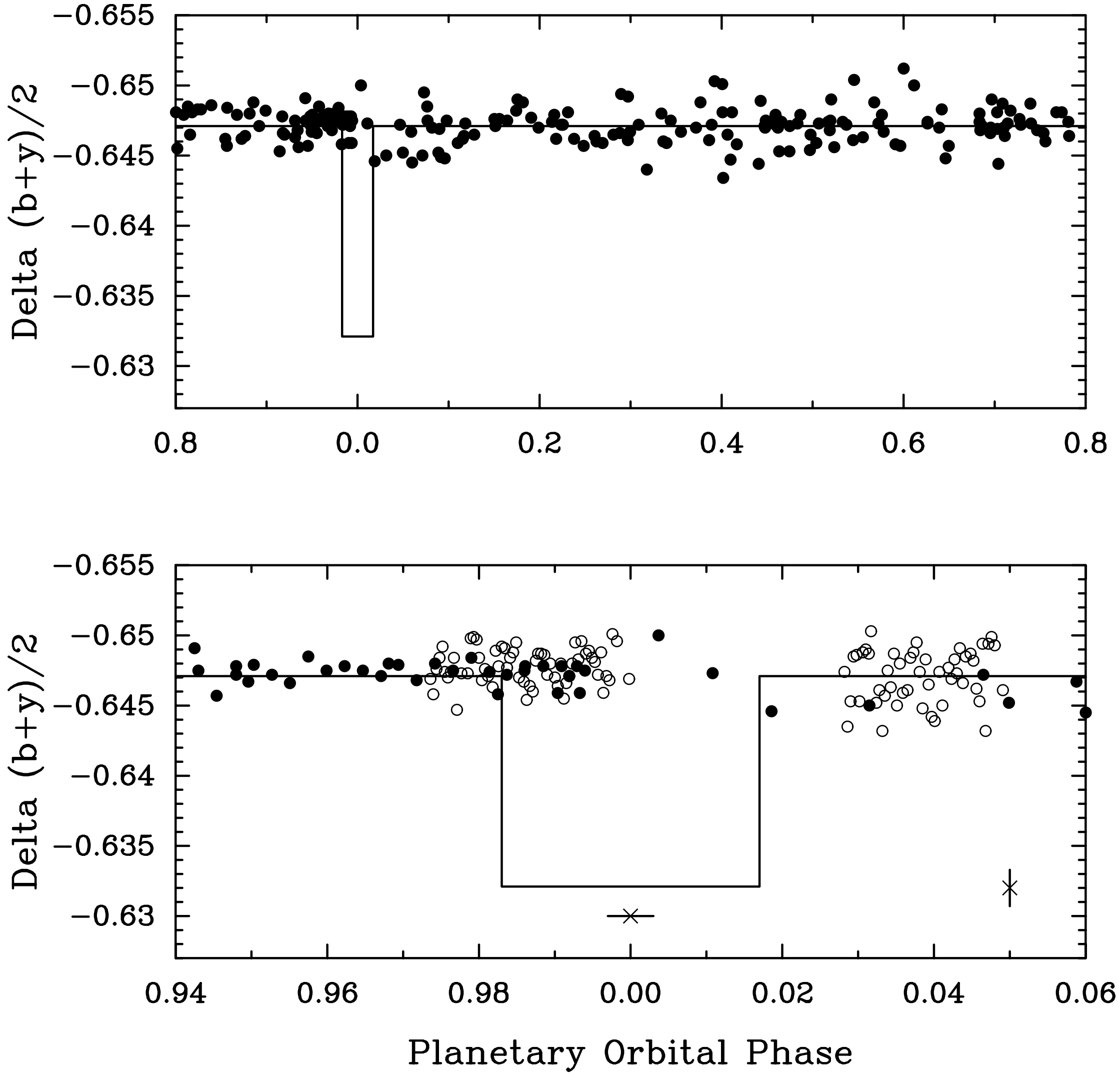

FIG. 4.—*Top*: Five seasons of nightly Strömgren $(b + y)/2$ differential magnitudes of 51 Peg plotted modulo the 4.2310 day orbital period of the companion. Phase 0.0 corresponds to the time of conjunction when the companion would transit the star for suitable orbital inclinations. A least-squares sine fit at the orbital period yields a semiamplitude of 0.00021 ± 0.00013 mag. The solid line shows the predicted drop in light for the transit of a $1.4R_{\rm Jup}$ planet across the 1.15 $R_\odot$ star. *Bottom*: Photometric observations of 51 Peg (*filled circles*) near the time of conjunction replotted with an expanded scale on the abscissa. Two additional nights of intensive observations with the 0.80 m APT from the 1997–1998 observing season have been added (*open circles*; see text). Although the probability of transits is 11%, our photometric observations show that they do not occur. The error bars have the same meaning as in Fig. 3.

close to $1.4R_{\rm Jup}$ (Guillot et al. 1997). Therefore, the photometric depth of a planetary transit across the 1.15 $R_\odot$ disk of 51 Peg would be 0.015 mag, somewhat deeper than estimated in Paper I. The duration of the transit would be ±0.017 phase units, or roughly 3.4 hr. The probability that transits should occur is 11%. The uncertainly in the time of midtransit, according to G. W. Marcy (1998, private communication), is only about 18 minutes, or 0.003 phase units, at this epoch. It is clear from Figure 4 that transits *do not* occur; the inclination of the orbit to our line of sight must be less than 84°.

4.2.2. Ca II *H and K Spectrophotometry*

In Paper I, we estimated the age of 51 Peg as ∼10 Gyr, based primarily on the long period (37 days), assumed to be rotation, in the 1989 observing season and also on its low Ca II flux. Fuhrmann et al. (1997), using isochrone-fitting results, found a younger age, 4 ± 2 Gyr, and Ford et al. (1998) estimated the age to be 7^{+4}_{-5} Gyr. Using our updated value of $\langle S \rangle = 0.150$, we estimate the age to be 7 Gyr.

Analysis of the recalibrated Ca II record reveals a slightly shorter rotation period, 36 days, in the 1989 observing season. Three additional possible but weak detections of rotational modulation were found in the 1980, 1984, and 1998 seasons with periods of 22, 23, and 22 days, respectively. If these three periods better indicate 51 Peg's mean rotation period (22 days), then they imply an age of ∼3 Gyr, much younger than the ∼10 Gyr listed in Paper I and the 7 Gyr estimated from $\langle S \rangle$. If the 36 day period is *also* due to rotation, $\langle P \rangle$ becomes 25 days, which suggests an age of 4–5 Gyr. Such short periods can be reconciled with the star's low $\langle S \rangle$ if 51 Peg is in a quiescent period, i.e., a Maunder minimum–like state (Baliunas & Jastrow 1990).

If the new, shorter rotation period is correct, then the age given in Paper I was overestimated, and 51 Peg is closer to (or younger than) solar age. Until the mean rotation period can be more accurately determined, our interim conclusion is that 51 Peg is closer to solar age than previously reported, ∼3–7 Gyr, within the range of the estimates made by Fuhrmann et al. (1997) and Ford et al. (1998).

4.3. *υ And* (= *HD* 9826 = *HR* 485)

The properties of υ And, discussed in Butler et al. (1997) and Paper II, are summarized in Table 1. We computed the absolute magnitude, luminosity, and radius in Table 1 with $V = 4.09$ and $B-V = 0.54$ from Mermilliod & Mermilliod (1994), $T_{\rm eff} = 6212$ K from Edvardsson et al. (1993), and a bolometric correction of -0.030 from Flower (1996). Properties of υ And's three planets and their orbits from Butler et al. (1999) are listed in Table 2. Paper II contained no photometry of υ And; here we present 2 yr of data collected since then. The two outer planets around υ And, with periods of 242 and 1269 days, are not addressed in this paper because the time span of our photometric and Ca II H and K observations is limited.

4.3.1. *Photometry*

The 121 nightly photometric observations taken with the 0.80 m APT over two observing seasons are summarized in Table 3. The yearly mean magnitudes in column (5) are differential $(b + y)/2$ magnitudes in the sense of υ And minus the comparison star HR 409 (F7 V). The standard deviations of single nightly observations are very small, indicating that the star is quite constant within each observing season. Periodogram analysis of the individual observing seasons and of the two seasons taken together reveal no significant periodicities between 1 and 100 days. The two yearly means differ by only 0.0002 mag, an insignificant amount. The 121 nightly observations are plotted in Figure 5 (*top*) with the orbital phase of the planetary companion computed from the ephemeris

$$\mathrm{JD}_{\rm conj} = 2{,}450{,}307.14 + 4.6170E \tag{3}$$

of Butler et al. (1999). A sine-curve fit to the data at the orbital period gives a semiamplitude of 0.00016 ± 0.00013 mag (Table 4), which is zero considering its uncertainty.

The portion of the phase curve near the time of conjunction is replotted in the bottom panel of Figure 5, where two additional nights of intensive observations (not included in

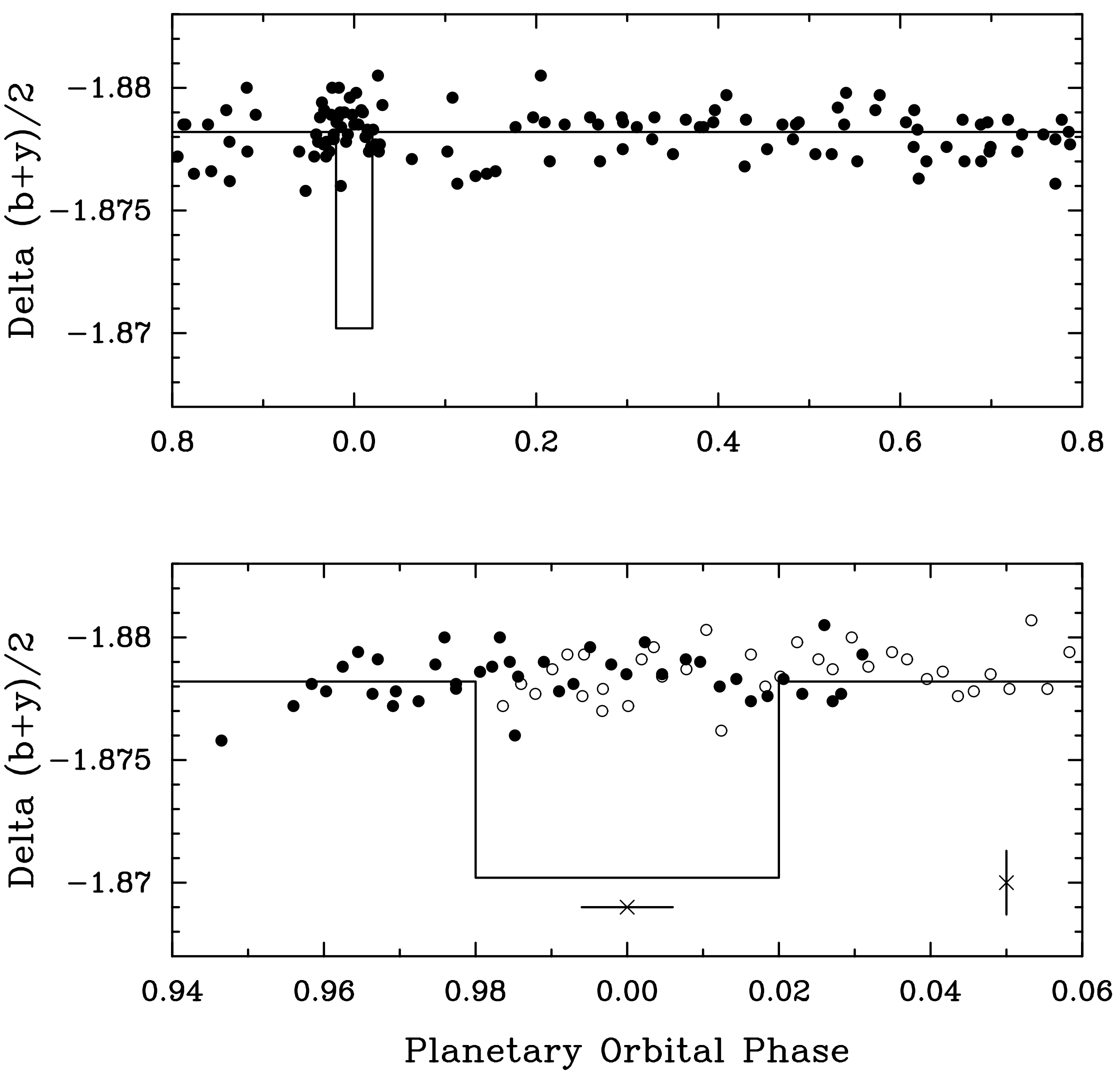

FIG. 5.—*Top*: Two seasons of nightly Strömgren $(b + y)/2$ differential magnitudes of υ And plotted modulo the 4.6170 day orbital period of the companion. Phase 0.0 corresponds to the time of conjunction when the companion would transit the star for suitable orbital inclinations. A least-squares sine fit at the orbital period yields a semiamplitude of 0.00016 ± 0.00013 mag. The solid line shows the predicted drop in light for the transit of a $1.4R_{\rm Jup}$ planet across the 1.60 $R_{\odot}$ star. *Bottom*: Photometric observations of υ And (*filled circles*) near the time of conjunction, replotted with an expanded scale on the abscissa. Two additional nights of intensive observations with the 0.80 m APT from the 1997–1998 observing season have been added (*open circles*; see text). The probability of transits is 13%, but our photometric observations show that they do not occur. The error bars have the same meaning as in Fig. 3.

the top panel of Figure 5 for reasons listed previously) acquired with the 0.80 m APT have been added. The solid line shows the drop in light that would result from a central transit of υ And b. A stellar radius of 1.6 $R_\odot$ and an orbital radius 0.059 AU permit transits to occur for orbital inclinations in the range $90° \pm 7.°2$. For a high-inclination orbit and a mass of the planet equal to the minimum mass, the planetary radius is approximately $1.4R_{\rm Jup}$ (Guillot et al. 1997). Therefore, the photometric depth of a transit would be 0.008 mag, while the duration would be ± 0.020 phase units, or 4.4 hr. The probability for such a transit is 13%. The uncertainty in the time of midtransit, according to G. W. Marcy (1998, private communication), is roughly 40 minutes, or 0.006 phase units. Our observations clearly *eliminate* the possibility of a transit, so the inclination of the orbit must be less than 83°.

4.3.2. Ca II *H and K Spectrophotometry*

The HK Project only began regular observations of υ And after the announcement of its possible planetary companion. Therefore, like the APT data, only a few years of observations are available. The star shows moderate year-to-year variability (Fig. 2) in Ca II H and K flux, although Butler et al. (1999) report no significant variation in the core of the Ca II 866.2 nm line.

Low-amplitude rotational modulation may be present in two observing seasons, with $P \sim 11$ days in 1996 and 19 days in 1998, with a grade of weak. A very weak 27 day period in 1997 is probably spurious. The star's $\langle S \rangle$ and $B-V$ suggest $P \sim 11.6$ days. Ford et al. (1998) argued that the rotation period should be even shorter, ~ 9 days, to match the observed $v \sin i$ of 9 km s^{-1} (Gray 1986). Butler et al. (1999) state that the difference of ~ 3 km s^{-1} in velocity renders them inconsistent; however, this ignores the possible effects of surface differential rotation, which could be sufficient to explain the difference. Ford et al. point out that $v \sin i$ measurements depend heavily on the choice of a macroscopic turbulence parameter and advise caution in its use, although Gray determined a macroturbulent velocity of 5.8 ± 0.8 km s^{-1}, which is consistent with stars of similar spectral type. A better determination of the rotation period may resolve the disagreement.

Our age determination of 4 Gyr based on $\langle S \rangle$ is consistent with that of 4 ± 1 Gyr by Fuhrmann et al. (1998) and the estimates of 2 ± 1 Gyr of Gonzalez (1998) and 3^{+2}_{-1} Gyr of Ford et al. (1998).

4.4. ρ^1 *Cnc* (= *HD 75732* = *HR 3522*)

The properties of ρ^1 Cnc are discussed in Butler et al. (1997) and Paper II and summarized in Table 1. We derived the absolute magnitude, luminosity, and radius in Table 1, with $V = 5.95$ and $B-V = 0.86$ from Mermilliod & Mermilliod (1994), $T_{\rm eff} = 5250$ K from Gonzalez & Vanture (1998), and a bolometric correction of -0.21 (Flower 1996). The properties of the planetary system, taken from Butler et al. (1997) and updated by G. W. Marcy (1998, private communication), are shown in Table 2. Butler et al. (1997) noted that the velocity residuals of the 14 day companion suggest a second companion with an orbital period greater than 8 yr and a minimum mass of $5M_{\rm Jup}$. Evidence for a dust disk surrounding ρ^1 Cnc has been reported by Dominik et al. (1998); from observations with the *ISO* satellite, they derive a total dust mass of $4 \times 10^{-5} M_\oplus$ in a disk ranging between 50 and 60 AU from the star.

4.4.1. *Photometry*

In Paper II, we reported the results of our first season of photometry of ρ^1 (55) Cnc, acquired with the 0.8 m APT, with respect to the comparison star ρ^2 (58) Cnc (G8 II–III). The other two comparison stars used that season were found to be low-amplitude variable stars and were replaced with 61 Cnc (F6 IV–V) and HD 74546 (F2) for our second and third observing seasons. Our new observations reveal that ρ^2 Cnc is also a low-amplitude variable. Therefore, in this paper we limit our discussion to the second and third observing seasons, summarized in Table 3. Differential magnitudes, still in the $(b + y)/2$ passband, have been computed with respect to 61 Cnc. The standard deviations in Table 3 show no evidence for intraseason variability of ρ^1 Cnc; the two yearly mean magnitudes also suggest no longer term variability.

The 210 nightly observations from these two observing seasons are plotted in Figure 6 (*top*) against the orbital phase of ρ^1 Cnc b computed with the ephemeris

$$\mathrm{JD_{conj}} = 2{,}450{,}206.04 + 14.649E \qquad (4)$$

of G. W. Marcy (1998, private communication). Fourier analysis of these data at the planetary period gives a semi-amplitude of 0.00011 ± 0.00009 mag (Table 4), a somewhat tighter constraint than we reported in Paper II, which used the old comparison star. Periodogram analysis of the data reveal no significant periodicities between 1 and 100 days.

The bottom panel of Figure 6 shows an expanded portion of the phase curve around the time of conjunction. Three additional nights of intensive observations from the 0.8 m APT (not included in the top panel of Figure 5 for reasons listed previously) have been added. The solid line shows the predicted drop in light for a transit of ρ^1 Cnc b. With a stellar radius of 0.96 $R_\odot$ and an orbital radius of 0.11 AU, the system could exhibit transits only over the inclination range $90° \pm 2.°3$. For a mass equal to the minimum mass, Guillot et al. (1997) compute a radius of $1.1R_{\rm Jup}$ for the companion. Therefore, the depth of a planetary transit would be 0.014 mag, a little larger than we estimated in Paper II. The duration of a central transit would be ± 0.007 phase units, or 4.5 hr. The probability of a transit is 4.1%. The uncertainty in the time of midtransit, according to G. W. Marcy (1998, private communication), is only about 38 minutes, or 0.002 phase units, at this epoch. Therefore, our observations clearly *rule out* any possibility of a transit; the inclination of the orbit must be less than 87.°7.

Recently, Trilling & Brown (1998) have succeeded in imaging the dust disk suspected by Dominik et al. (1998) with the cooled coronagraph of the 3 m Infrared Telescope Facility (IRTF) on Mauna Kea. They measure its inclination to be $27°^{+8°}_{-11°}$. This low inclination is consistent with the lack of observed photometric transits. If the planet's orbit lies in the same plane, its mass is $1.9^{+1.1}_{-0.4} M_{\rm Jup}$, well below the mass of brown dwarfs.

4.4.2. Ca II *H and K Spectrophotometry*

The Ca II record (Fig. 2) shows significant year-to-year changes, suggesting cyclic activity with a maximum in 1995. Rotation was confidently detected in five seasons (Table 5): 1984 (39 days), 1994 (43 days), 1995 (41 days), 1997 (37 days), and 1999 (35 days), with an average of 39 days and a grade of confirmed. The rotational velocity estimated from the observed period is consistent with the measured value of $v \sin i$ and the predicted rotation period of 42 days based

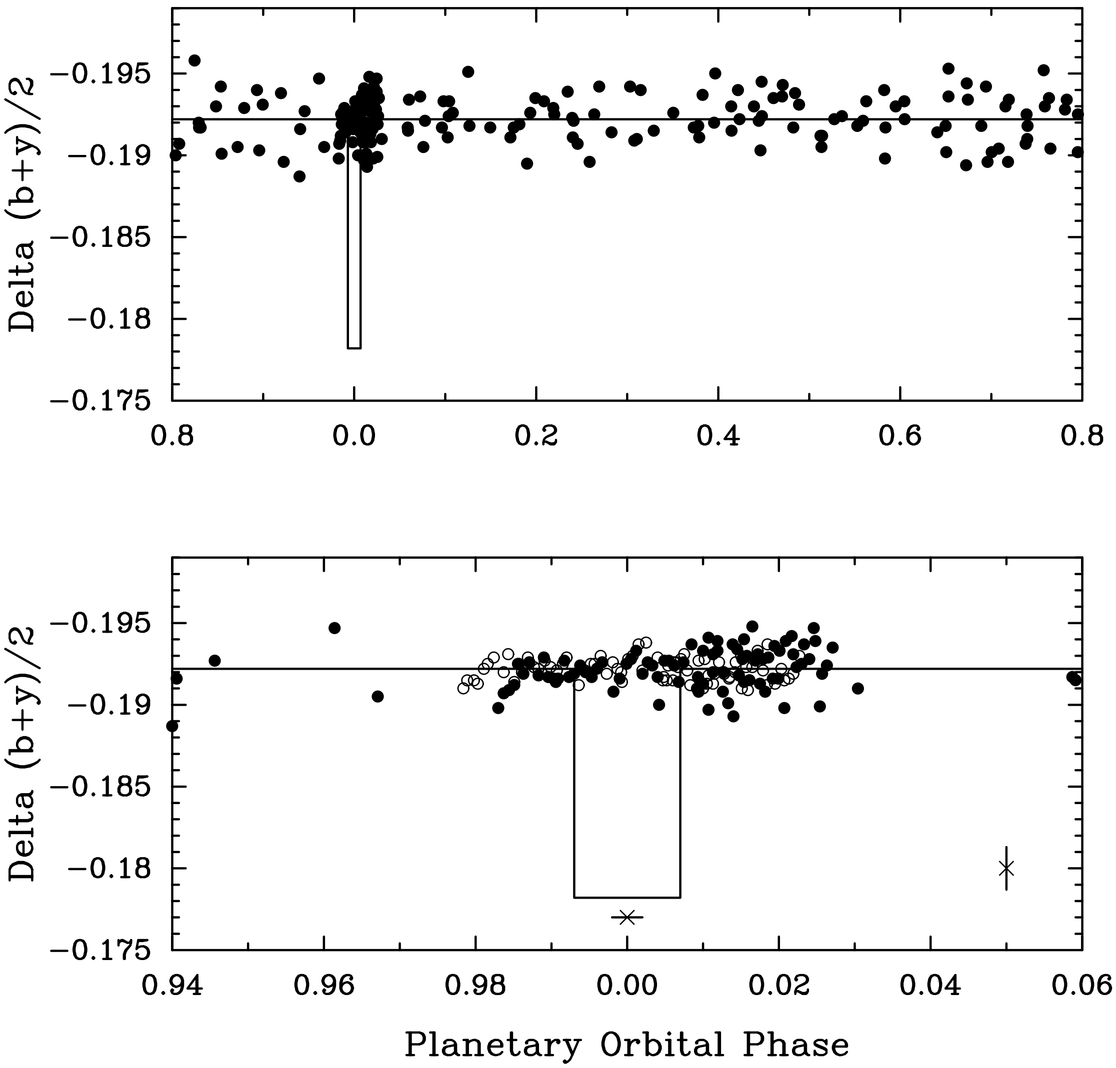

FIG. 6.—*Top*: Two seasons of nightly Strömgren $(b + y)/2$ differential magnitudes of ρ^1 Cnc plotted modulo the 14.649 day orbital period of the companion. Phase 0.0 corresponds to the time of conjunction when the companion would transit the star for suitable orbital inclinations. A least-squares sine fit at the orbital period yields a semiamplitude of 0.00011 ± 0.00009 mag. The solid line shows the predicted drop in light for the transit of a $1.1 R_{\rm Jup}$ planet across the 1.00 $R_\odot$ star. *Bottom*: Photometric observations of ρ^1 Cnc (*filled circles*) near the time of conjunction replotted with an expanded scale on the abscissa. Three additional nights of intensive observations with the 0.80 m APT from the 1997–1998 observing season have been added (*open circles*; see text). The probability of transits is 4.2%, but our photometric observations clearly show that they do not occur. The error bars have the same meaning as in Fig. 3.

on $\langle S \rangle$. Both $\langle P \rangle$ and $\langle S \rangle$ imply that the star is solar age (4–5 Gyr).

Gonzalez & Vanture (1998) have reduced their age estimate to 4 ± 3 Gyr. Fuhrmann et al. (1998; their Fig. 5) place ρ^1 Cnc below the zero-age main sequence (ZAMS), and suggest that the star is very young, but they assign to their age an uncertainty that extends to the age of the Sun and overlaps the revised value of Gonzalez & Vanture (1998). Ford et al. (1998) estimate the age to be 8^{+7}_{-8} Gyr. The age determined from $\langle S \rangle$ and $\langle P \rangle$, 4.5 Gyr, is consistent with the ages from evolutionary-track comparisons, given the large uncertainties.

4.5. *ρ CrB* (= *HD 143761* = *HR 5968*)

The discovery of a companion to ρ CrB was announced by Noyes et al. (1997a, 1997b). The planet possesses a minimum mass of $1.1 M_{\rm Jup}$ and moves in a circular orbit with a period of 40 days. The properties of this old G0–2 V star, based in part on the new parallax from the *Hipparcos* catalogue, are reviewed by Noyes et al. (1997a) and are summarized in our Table 1. The properties of the planetary companion and its orbit from the same source are given in Table 2, with updates from R. W. Noyes (1998, private communication).

4.5.1. *Photometry*

Since 1993, we have accumulated 404 group observations with the 0.75 m APT. Results from the six observing seasons are given in Table 3. Yearly mean magnitudes are differential $(b + y)/2$ magnitudes in the sense of ρ CrB minus π CrB (HD 140716), the best of our three comparison stars. The standard deviation of a single group observation from the yearly mean for each observing season ranges from 0.0009 to 0.0017 mag and is consistent with a constant star. Periodogram analysis of the individual observing seasons and of the six seasons taken together reveal no significant periodicities in the range 1–100 days.

The photometric results in Table 3 show both intra- and interseasonal photometric stability in ρ CrB. The range in the yearly mean magnitudes is insignificant, only 0.0003 mag over the first four seasons. Although ρ^1 CrB is apparently brighter by about 0.001 mag in the fifth and sixth seasons, we suspect instead a fading of the comparison star, π CrB. The radius of π CrB, estimated from the *Hipparcos* parallax and the $B-V = 1.06$ color index given in Mermilliod & Mermilliod (1994), is 9–10 $R_\odot$ and is thus consistent with the gG9 classification listed in the Bright Star Catalogue and our own spectral classification of K0 III. A significant percentage of late G giants and K giants used as comparison stars in our long-term program of precision photometry are low-amplitude variable stars (Fekel & Henry 1998). While we cannot confirm the fading of π CrB because of even greater photometric variations in the other two comparison stars, the nonvariability of ρ CrB is supported by the comparative flatness of its Ca II record (Fig. 1). The standard deviation of the yearly mean magnitudes from column (5) of Table 3 from the mean of the means, given as 0.0001 mag in Table 4, does not include the results of the fifth and sixth observing seasons.

The photometric observations from the six seasons are plotted modulo the planetary orbital period in the top panel of Figure 7. Normally, one observation is acquired per night, but the 404 observations include 54 taken on the three nights, JD 2,450,977–JD 2,450,979. Zero phase is the time of inferior conjunction of the planetary companion (the predicted time of planetary transit for favorable inclinations) and was computed with the updated ephemeris

$$\mathrm{JD_{conj}} = 2{,}450{,}977.79 + 39.90E \qquad (5)$$

from R. W. Noyes (1998, private communication). The individual observations in seasons 1, 2, 5, and 6 have been adjusted so that their yearly means equal those of seasons 3 and 4. Fourier analysis of these data at the planetary period gives a semiamplitude of 0.00011 ± 0.00009 mag (Table 4), so any real light variation at this period must be extremely small.

The portion of the phase curve near the time of conjunction is replotted in the bottom panel of Figure 7, with an

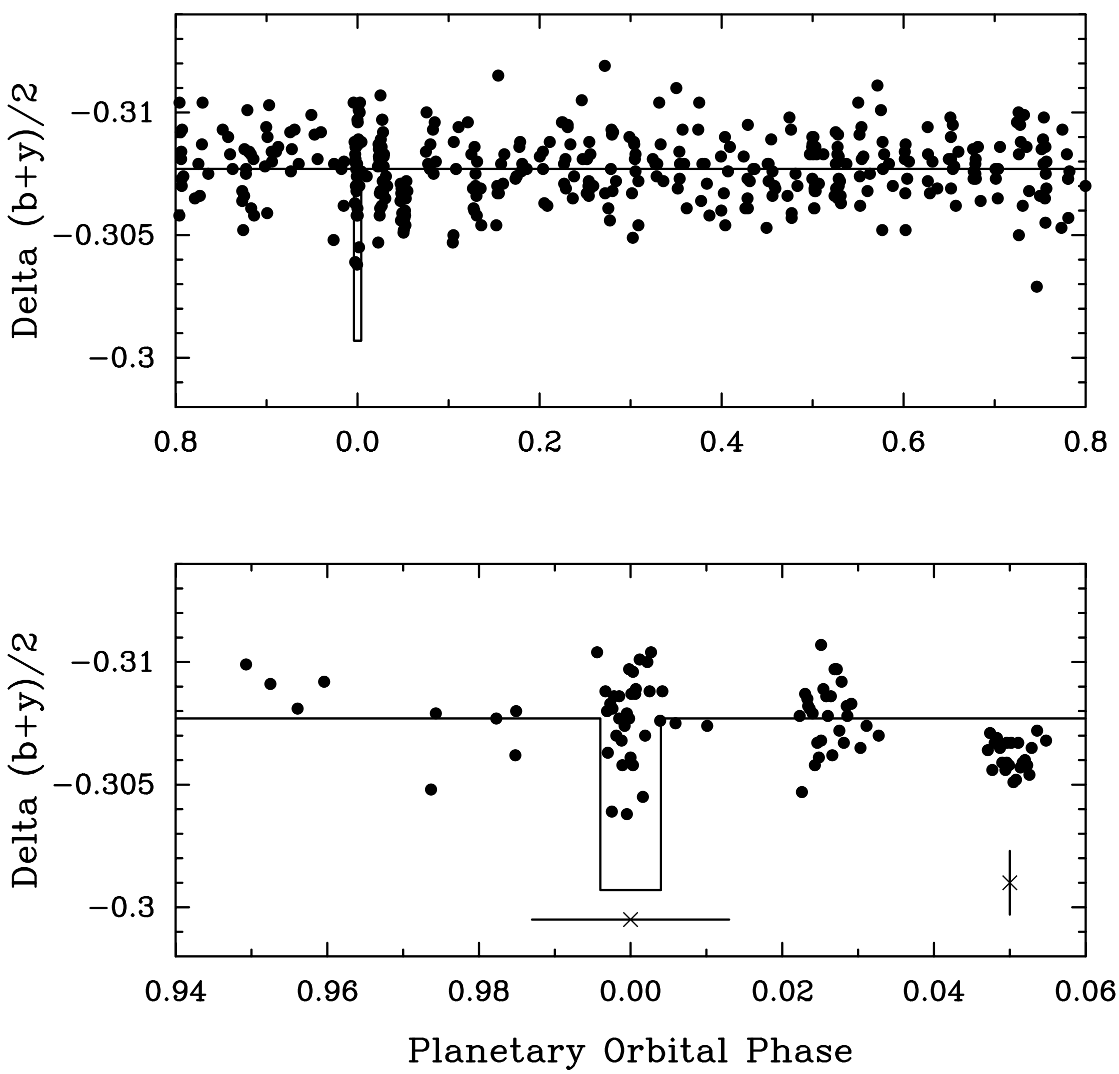

FIG. 7.—*Top*: Six seasons of nightly Strömgren $(b + y)/2$ differential magnitudes of ρ CrB plotted modulo the 39.90 day orbital period of the companion. Phase 0.0 corresponds to the time of conjunction when the companion would transit the star for suitable orbital inclinations. A least-squares sine fit at the orbital period yields a semiamplitude of 0.00011 ± 0.00009 mag. The solid line shows the predicted drop in light for a $1.1 R_{\mathrm{Jup}}$ planet across the $1.31 R_\odot$ star. *Bottom*: Photometric observations of ρ CrB near the time of conjunction, replotted with an expanded scale on the abscissa. The observations show no evidence of a transit. However, since the time of transit is still uncertain by about 0.013 phase units and the duration of the transit could be shorter than the indicated central transit, our observations do not completely rule out the possibility of a transit, although their probability is only 2.6%. The error bars have the same meaning as in Fig. 3.

expanded scale on the abscissa. The solid line shows the drop in light that would result from a central transit of ρ CrB b. For such a transit to occur, the inclination of the orbit would have to be $90° \pm 1.5°$, and the mass of the planet $1.1M_{\rm Jup}$. The radius of the planet, estimated from the models of Guillot et al. (1997), would then be $\sim 1.1R_{\rm Jup}$, including the effects of insolation from the star. This planetary radius, combined with the stellar radius of 1.31 $R_\odot$ for ρ CrB, gives a predicted transit depth of 0.007 mag, easily observable at our precision of 0.001 mag for a single observation. With an orbital radius of 0.23 AU, the full duration of a central transit of ρ CrB b would be ± 0.004 phase units, or 8.0 hr. The geometric probability that transits of the planet occur is 2.6%. One of our three nights of intensive photometric monitoring (not included in the top panel of Figure 5 for reasons listed previously) around the conjunction completely covers the predicted transit window and shows no evidence of a transit. However, the uncertainty in the predicted time of transit from R. W. Noyes (1998, private communication) is 0.5 days, or 0.013 phase units. Therefore, given that the transit could be shorter than the 8 hr calculated for a central passage, our data do not rule out the possibility of a transit.

We note that the *Hipparcos* catalogue gives an astrometric orbital solution for ρ CrB with a period of 78.0 ± 0.9 days, which is twice the planetary orbital period, within the errors, of Noyes et al. (1997a). The semimajor axis of the photocentric orbit is given as 2.34 ± 0.86 mas, and the orbital inclination is $104° \pm 17°$. However, the planetary companion discovered by Noyes et al. should produce an astrometric wobble of only 0.01 mas or so for likely values of the inclination and corresponding mass of the planet. Therefore, the radial-velocity variations in ρ CrB predicted by the *Hipparcos* results should be 100 times larger than those observed. Furthermore, since the size of the orbit in the *Hipparcos* catalogue is only 2.7 times its uncertainty, we conclude that the *Hipparcos* results are spurious.

4.5.2. Ca II *H and K Spectrophotometry*

The Ca II record for ρ CrB is plotted in Figure 1. The predicted rotation period is 19.9 days; five detections of rotation have been made over 18 yr. The average period is 19 days, with a grade of confirmed; periods range from 17.2 to 19.8 days (Table 5). The rotation period and $\langle S \rangle$ both suggest an age of ~ 6 Gyr, lower than that of Gonzalez (1998; 11 ± 2 Gyr), Fuhrmann et al. (1998; 10 ± 2 Gyr), and Ford et al. (1998; 14 ± 2 Gyr). Fuhrmann et al. (1998) point out that the predicted rotation period combined with previously determined $v \sin i$ values of 1.0–1.5 km s^{-1} suggests a low inclination (less than 35°), which is consistent with the nondetection of a photometric transit. The larger $v \sin i$ value found here (2.1 ± 0.5 km s^{-1}) is within two standard deviations of the previous range and is also consistent with the observed rotation period. The new, larger value of $v \sin i$ yields a larger inclination (greater than 52°), still consistent with the observed lack of transits.

4.6. *70 Vir (= HD 117176 = HR 5072)*

The companion to 70 Vir was discovered by Marcy & Butler (1996); stellar properties were discussed in that paper and in Paper I and are summarized in Table 1. We computed the absolute magnitude, luminosity, and radius in Table 1 with $V = 4.97$ and $B-V = 0.71$ from Mermilliod & Mermilliod (1994), $T_{\rm eff} = 5488$ K from Blackwell & Lynas-Gray (1994), and a bolometric correction of -0.132 from Flower (1996). Table 2 summarizes the properties of the planetary system from Marcy & Butler (1996) and G. W. Marcy (1998, private communication).

4.6.1. *Photometry*

In Paper I, we presented photometric observations of 70 Vir over three observing seasons; here we extend our coverage to six seasons. The 387 nightly observations from these six seasons are summarized in Table 3 and plotted in Figure 8 (*top*) against orbital phase of the companion computed with the ephemeris

$$\mathrm{JD}_{\rm conj} = 2{,}450{,}171.94 + 116.67E \, , \qquad (6)$$

where the time of conjunction was derived from an updated orbital solution (G. W. Marcy 1998, private communication). Differential magnitudes are in the $(b + y)/2$ passband and are computed with respect to the comparison star 71 Vir (K0 III). The individual observations in seasons 2–6 have been adjusted so that their yearly means equal the mean of the first observing season. Fourier analysis of the adjusted data at the 116.67 day period gives a semi-amplitude of 0.00020 ± 0.00011 (Table 4), in agreement with our results in Paper I. Periodogram analyses of the data reveal no significant periodicities between 1 and 200 days. The standard deviations of the nightly observations in column (6) of Table 3 are also consistent with short-term nonvariability. The yearly mean magnitudes imply a gradual brightening of 70 Vir of over 0.002 mag, but we suspect at least some of this to be a dimming of the comparison star. Therefore, the long-term variation in 70 Vir, given in Table 4 as 0.0010 mag, is an upper limit.

The bottom panel of Figure 8 shows a portion of the light curve expanded around the time of conjunction. For a stellar radius of 1.93 $R_\odot$ and an orbital radius of 0.43 AU, transits of the companion could occur over a range of inclinations $90° \pm 1.2°$. Guillot et al. (1997) compute the radius of the companion to be $\sim 1.05R_{\rm Jup}$ for a mass equal to the minimum mass, so the photometric depth of a planetary transit would be only about 0.003 mag. For a central transit, the duration would be roughly ± 0.003 phase units, or a total of 18.5 hr. The solid line in Figure 8 illustrates the depth and duration of such a transit. Our observations cover the predicted time of midtransit, yet no transit is seen. Since the uncertainty in the time of midtransit is 0.003 phase units, or about half of the transit duration, we cannot completely rule out the possibility of a transit. The geometric probability for transits is 2.1%.

4.6.2. Ca II *H and K Spectrophotometry*

The long-term Ca II flux record is plotted in Figure 2. There is a downward trend in *S* with time, but no significant variability. The expected rotation period estimated from the mean level of activity is 35.8 days; rotational modulation was possibly detected during the 1997 and 1998 observing seasons with periods of 29 and 31 days, respectively, but the period determination is listed as weak (Table 5).

The age inferred from $\langle S \rangle$ is ~ 8 Gyr and agrees with previous values of 8 ± 1 Gyr (Gonzalez 1998) and 7 ± 2 Gyr (Fuhrmann et al. 1997). The observed rotation periods suggest a younger age, ~ 4 Gyr, but the weak detection of rotation makes this estimate doubtful.

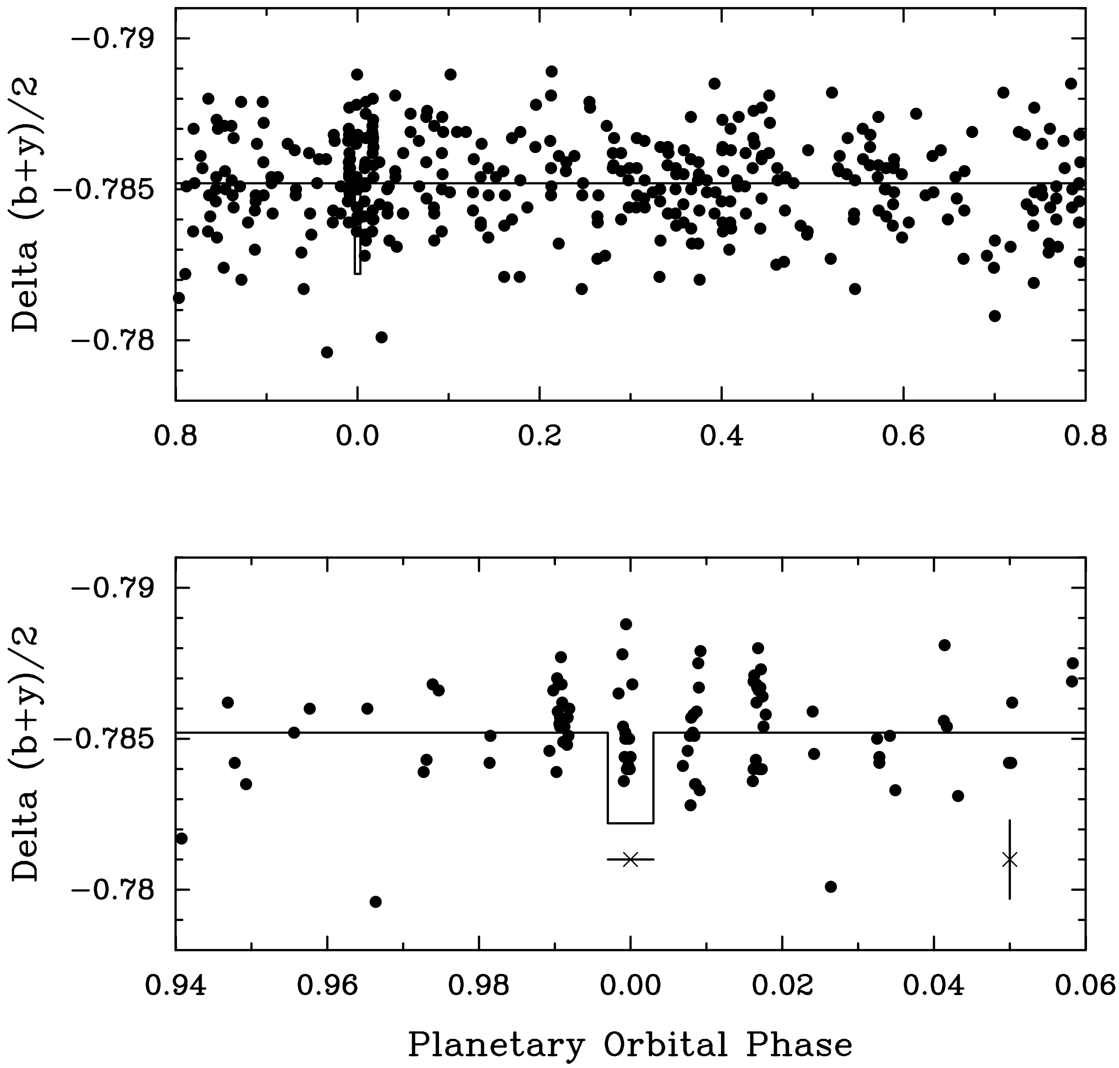

FIG. 8.—*Top*: Six seasons of nightly Strömgren $(b + y)/2$ differential magnitudes of 70 Vir plotted modulo the 116.67 day orbital period of the companion. Phase 0.0 corresponds to the time of conjunction when the companion would transit the star for suitable orbital inclinations. A least-squares sine fit at the orbital period yields a semiamplitude of 0.00020 ± 0.00011 mag. The solid line shows the predicted drop in light for the transit of a $1.05 R_{\rm Jup}$ planet across the 1.93 $R_{\odot}$ star. *Bottom*: Photometric observations of 70 Vir near the time of conjunction, replotted with an expanded scale on the abscissa. The geometric probability of transits is 2.1%. Our observations cover the predicted time of midtransit and do not reveal any dimming. Since the uncertainty in the time of transit is 0.003 phase units or about half of the transit duration, our photometric observations do not completely rule out the possibility of a transit. The error bars have the same meaning as in Fig. 3.

4.7. *16 Cyg B (= HD 186427 = HR 7504)*

The companion to 16 Cyg B, with a minimum mass of $1.5 M_{\rm Jup}$ and an eccentric 800 day orbit, was discovered by Cochran et al. (1997). This star is the slightly fainter component of the visual binary ADS 12815, composed of two early G dwarfs separated by 39″. Both components have properties very similar to the Sun and were among the four stars rated as the closest solar analogs at the Lowell Observatory Workshop on Solar Analogs held in 1997 October (Hall 1998). Cochran et al. (1997) review the properties of 16 Cyg B, and these are summarized in our Table 1. We computed the absolute magnitude, luminosity, and radius, with $V = 6.21$ and $B - V = 0.66$ from Mermilliod & Mermilliod (1994), $T_{\rm eff} = 5760$ K from Friel et al. (1993), and a bolometric correction of -0.098 (Flower 1996). Properties of the planetary system from Cochran et al. (1997) and G. W. Marcy (1998, private communication) are given in Table 2.

4.7.1. *Photometry*

We have no photometry of 16 Cyg B because of difficulties the 0.8 m APT experienced in acquiring and isolating the fainter component of the visual binary system.

4.7.2. Ca II *H and K Spectrophotometry*

The Ca II record of 16 Cyg B is plotted in Figure 2. Low-amplitude variability is seen from season to season. The expected rotation period estimated from the mean activity level is 27.4 days (Table 5). Only two weak detections of rotational modulation are evident in 1996 (38 days) and 1997 (25 days), so the period is poorly determined. The $v \sin i$ value is consistent with the rotation period. The age inferred from $\langle S \rangle$ is ~ 6 Gyr for 16 Cyg B; the mean activity of 16 Cyg A ($\langle S \rangle = 0.151$) results in an estimated age of 7 Gyr. These are close to the lower limit of ages derived by Gonzalez (1998; 9 ± 2 for both 16 Cyg A and 16 Cyg B) and

Fuhrmann et al. (1998; 8 ± 1 Gyr for 16 Cyg A and 8 ± 2 Gyr for 16 Cyg B).

4.8. *47 UMa* (= *HD 95128* = *HR 4277*)

Butler & Marcy (1996) announced the presence of a planet orbiting 47 UMa and reviewed the properties of the star. Further discussion of the stellar properties can be found in Paper I and in Fuhrmann et al. (1997). These are summarized in Table 1, where we compute the absolute magnitude, luminosity, and radius, with $V = 5.05$ and $B-V = 0.61$ from Mermilliod & Mermilliod (1994), $T_{\rm eff} = 5882$ K from Edvardsson et al. (1993), and a bolometric correction of -0.067 (Flower 1996). Properties of the planet and its orbit from Butler & Marcy (1996) and G. W. Marcy (1998, private communication) are summarized in our Table 2.

4.8.1. *Photometry*

In Paper I, we presented photometric observations from the early part of our first observing season obtained with the 0.75 m APT. We now have 242 observations from three seasons; these are summarized in Table 3. Yearly mean magnitudes are differential $(b + y)/2$ magnitudes in the sense of 47 UMa minus HR 4264 (K2 III). The standard deviations given in column (6) of Table 3 are fairly small, indicating that 47 UMa is constant within each season. The mean magnitudes indicate a slight change of 0.0008 mag over 3 yr owing to photometric changes in the comparison star. The other two comparison stars were more variable than HR 4264 and were replaced in season 2. The two new comparison stars show better stability than HR 4264, but HR 4264 is the only comparison star that was used in all three observing seasons. Therefore, the long-term standard deviation of 0.0004 mag given in Table 4 is an upper limit.

The 242 nightly observations are plotted in the top panel of Figure 9 against the orbital phase of the planet computed with the ephemeris

$$\mathrm{JD}_{\rm conj} = 2{,}449{,}099 + 1035E\ , \tag{7}$$

where the time of conjunction has been derived from an updated orbital ephemeris (G. W. Marcy 1998, private

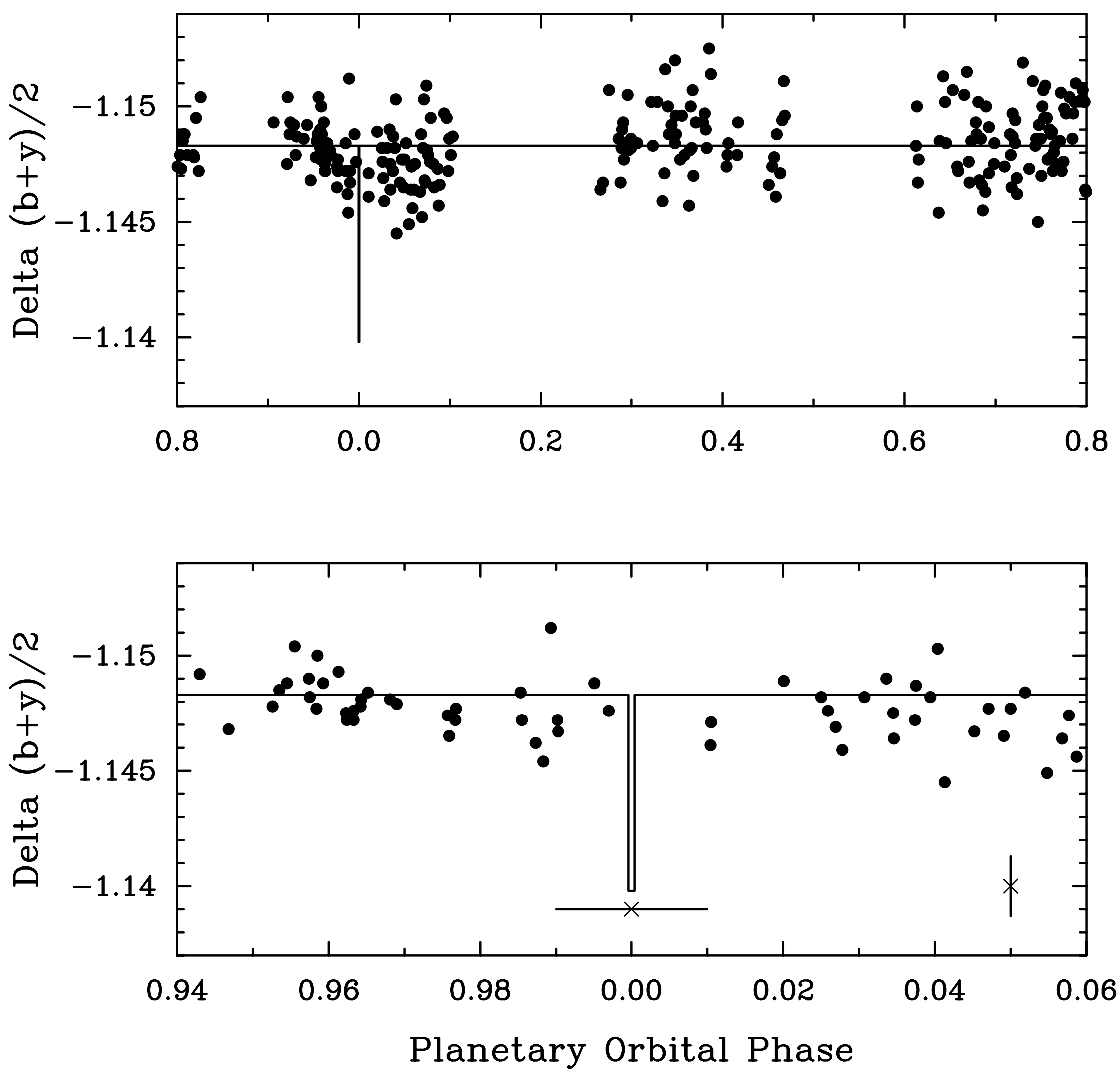

FIG. 9.—*Top*: Three seasons of nightly Strömgren $(b + y)/2$ differential magnitudes of 47 UMa plotted modulo the 1035 day orbital period of the companion. Phase 0.0 corresponds to the time of conjunction when the companion would transit the star for suitable orbital inclinations. The phases of the observations are not well distributed because of the orbital period; the season centered near phase 0.0 is our first observing season. The solid line shows the predicted drop in light for a transit of a $1.1R_{\rm Jup}$ planet across the 1.22 $R_\odot$ star. *Bottom*: Photometric observations of 47 UMa near the time of conjunction, replotted with an expanded scale on the abscissa. The uncertainty in the time of transit is roughly 0.01 phase units, so our observations do not rule out the possibility of transits; the geometric probability for them is only 0.27%. The error bars have the same meaning as in Fig. 3.

communication). The phases of the observations are not well distributed because of the long orbital period; our data extend over slightly less than one complete orbit. The group of points centered near phase 0.0 is our first observing season. Fourier analysis on the planetary orbital period gives a semiamplitude of 0.00048 ± 0.00013 mag (Table 4), but this apparent variation is likely from variability in the comparison star, as discussed above. Therefore, the semiamplitude on the planetary orbital period is an upper limit to variability in 47 UMa.

The portion of the phase curve near the time of conjunction is replotted in the bottom panel of Figure 9. The solid line shows the drop in light for a central transit of the planet across the 1.22 $R_{\odot}$ disk of 47 UMa. For a mass equal to the minimum mass, the radius of the planet computed from the models of Guillot et al. (1997) would be $1.1 R_{\rm Jup}$, which gives a transit depth of 0.0085 mag. The duration of a central transit would be ± 0.00043 phase units, or a total of about 22.5 hr. At the orbital radius of 2.1 AU, however, planetary transits would occur only for inclinations in the range 90° $\pm$ 0°.16. Their geometric probability is only 0.27%. The predicted time of conjunction occurs near the middle of our first observing season. The uncertainty in the time of conjunction is roughly ± 10 days, or ± 0.01 phase units. Therefore, our photometry clearly does not rule out the possibility of transits, although their probability is very low.

4.8.2. Ca II *H and K Spectrophotometry*

The Ca II record for 47 UMa is plotted in Figure 2. The star's activity has been increasing over the last 6 yr. One marginal detection of a weak 71 day period comes from the 1994 season. This is inconsistent with the predicted period of 21 days. However, a 71 day period is marginally consistent with the observed $v \sin i$ (2 ± 1 km s^{-1}) and stellar radius derived from *Hipparcos* parallax if 47 UMa has evolved off the main sequence and begun to spin down.

If 47 UMa is on the main sequence, its age inferred from $\langle S \rangle$ is 6 Gyr (Table 6), in agreement with other estimates of 8 ± 2 Gyr (Gonzalez 1998) and 6.5 Gyr (Ng & Bertelli 1998).

4.9. *Gl 411 (= HD 95735 = Lalande 21185)*

Gatewood (1996) reported accelerations in the astrometric motion of Gl 411 that indicate the presence of a planetary system. The shorter period component of the accelerations implies a planet with a probable mass of $0.9 M_{\rm Jup}$ and a 5.8 yr circular orbit. If confirmed, this would be the first example of an extrasolar planetary system found via astrometric means.

As the fourth-closest stellar system to the Sun (Henry et al. 1997b), Gl 411 has been a prime target of astrometric searches for planetary companions for nearly 50 yr (Gatewood et al. 1992 and references therein). Perturbations in its proper motion with periods of 8.0 yr (Lippincott 1960) and 22 yr (Hershey & Lippincott 1982) have been reported but never confirmed. Companions have also been sought unsuccessfully with speckle interferometry (Henry & McCarthy 1990) and radial-velocity techniques (Marcy & Benitz 1989). An old disk star (Eggen 1979), Gl 411 is an M2 dwarf (Henry, Kirkpatrick, & Simons 1994) with a metallicity slightly less than solar (Mould 1978). Determinations of its effective temperature range from 3320 to 3428 K (Mould 1978; Berriman, Reid, & Leggett 1992; O'Neal & Neff 1997). The star was among the 91 included in Wilson's (1978) 12 yr study of Ca II variations in lower main-sequence stars and continues to be observed as the coolest star in the HK Project (Baliunas et al. 1995). Ca II H and K fluxes are lower than in the more active dMe stars, but flaring activity has been observed in the H and K lines by Donahue et al. (1986). Giampapa et al. (1996) have also detected coronal X-rays with *ROSAT*. The basic properties of the star are listed in Table 1. We computed the absolute magnitude, luminosity, and radius, with $V = 7.50$ and $B-V = 1.51$ from Mermilliod & Mermilliod (1994), $T_{\rm eff} = 3350$ K from O'Neal & Neff (1997), and a bolometric correction of -1.178 from Flower (1996). Properties of the inferred planetary orbit from Gatewood (1996) are given in Table 2.

4.9.1. *Photometry*

After Gatewood's (1996) announcement, we placed Gl 411 on the observing menu of the 0.4 m APT. We have observations from two observing seasons, a much shorter time span than the orbital period reported for the companion. Yearly means of the photometry are given in Table 3, along with their errors. Johnson *B* and *V* differential magnitudes are in the sense of Gl 411 minus the comparison star HD 95485 ($V = 7.3$, F0) and have been combined into a single $(B + V)/2$ passband to improve precision. The observed standard deviations of single observations from the yearly means are between 0.003 and 0.004 mag and so are consistent with the nonvariation of both stars as measured with this telescope. There is no evidence in the data for short-term flaring activity. Periodogram analysis reveals no significant periods in the range 1–100 days. The two yearly means are identical to within 0.0002 mag; the standard deviation of the two yearly means from their mean is 0.0001 mag (Table 4). Therefore, we find no evidence so far of any photometric variability in Gl 411. For comparison, Weis (1994) found significant long-term photometric variability in 21 of 43 dwarf M stars, a few of which were dMe stars. If the 5.8 yr orbit is confirmed, the probability that transits occur for the companion is only about 0.078%.

Although the reported planet orbiting Gl 411 was detected astrometrically, hypothetically, a change in the presence of surface inhomogeneities can introduce photocenter wander, which could mimic astrometric accelerations. This effect would also increase with decreasing distance (2.55 pc for Gl 411). Surface inhomogeneities producing flux variations of 0.1% would result in a photocenter motion of ~ 10 μas at a distance of 1 pc, or ~ 4 μas at the distance of Gl 411; the latter is the intended precision of the *Space Interferometry Mission* astrometric grid. Our photometric time series does not yet cover one orbital period, but the year-to-year variability suggests that, on a timescale of 6 yr, Gl 411 would vary with an amplitude of less than 0.001 mag (0.1%). Nonetheless, the effects of activity on precision astrometric measurements need to be considered in the search for planetary candidates in astrometric data.

4.9.2. Ca II *H and K Spectrophotometry*

The Ca II H and K record of Gl 411 is shown in Figure 1. Baliunas et al. (1995) characterize the long-term behavior as variable (i.e., significant variability without pronounced periodicity). The Ca II flux record presented here is also classified as variable.

Donahue et al. (1986) inferred a rotation period of 47 days from the 1981 observing season. Nine determinations of rotational modulation have been made during eight observing seasons, with a mean period of 45 days. However, two groups of periods are listed in Table 5. Five very confident periods lie in the range 51–60 days (the 51 day period is from the 1981 observing season). The remaining four periods range from 30 to 35 days. A large range in period may be explained by surface differential rotation. Both groups of periods are consistent with the small and uncertain $v \sin i \simeq 1.4 \pm 1$ km s^{-1}.

5. GENERAL DISCUSSION

5.1. *Photometry in Support of the Planetary Hypothesis*

For the six planetary candidates with orbital periods of less than 4 months (τ Boo b, 51 Peg b, υ And b, ρ^1 Cnc b, ρ CrB b, and 70 Vir b), we have shown that no significant stellar photometric variations occur on the planetary orbital periods to a precision of 0.0001 or 0.0002 mag (Table 4). For 47 UMa, we have shown that photometric variations on the 2.8 yr planetary period are similarly small, although our precision is adversely affected by variability of the comparison star. Our two seasons of photometry of Gl 411 cover only 25% of the suspected 6 yr orbit, but so far we see no detectable long-term photometric variations to a precision of 0.0001 mag.

Our photometric observations are sufficient to rule out surface magnetic activity as the cause of the observed radial-velocity variations for all the stars except Gl 411 and 16 Cyg B. The radial-velocity amplitudes for the stars range from 46 to 463 m s^{-1} (Table 2). Saar, Butler, & Marcy (1998) concluded (see the right panel of their Fig. 1) that F, G, and K dwarfs generally produce intrinsic (nonreflex) radial-velocity variations greater than about 50 m s^{-1} only if they have Ca II emission ratios (log $R'_{\rm HK}$) of around -4.5 or larger. However, all of our stars, except Gl 411, have log $R'_{\rm HK}$ values substantially *less* than -4.5 (Table 6). In addition, Baliunas et al. (1998) have shown that Sun-like stars with log $R'_{\rm HK}$ greater than -4.5 *always* have detectable photometric variations with standard deviations of 0.005 mag or larger (see their Fig. 10). For example, Queloz et al. (1999) found that radial-velocity variations with an amplitude of 80 m s^{-1} in the G0 dwarf HD 166435 were produced by starspots that generated a photometric amplitude of 0.06 mag. Therefore, surface magnetic activity sufficient to produce a measurable radial-velocity signal will also produce significant photometric variations. The lack of photometric variations to the precisions established above argues that the radial-velocity variations are *not* caused by surface magnetic activity.

The extent to which we can use the lack of photometric variations to exclude nonradial oscillations as the source of the radial-velocity variations is not as clear. Gray & Hatzes (1997) and Hatzes & Cochran (1998) review some of the difficulties in predicting expected photometric variations arising from various pulsation modes. While photometric variations are expected in many situations, they suggest that some pulsation modes might be capable of mimicking reflex radial-velocity variations and yet result in photometric variations below our level of detection. In particular, they speculate that geometric effects of the oscillations might be cancelled by out-of-phase temperature variations, producing little net change in light. However, detailed physical models of these processes do not exist, and observational confirmation (i.e., observed line-profile variations coincident with a high level of photometric nonvariability) is lacking. Recent high-resolution spectroscopic observations of 51 Peg (Gray 1998; Hatzes et al. 1998; Brown et al. 1998) and τ Boo (Brown et al. 1998; Hatzes & Cochran 1998) find no evidence for line-profile variations, in agreement with our stringent limits on photometric variations. Moreover, classes of stars that *do* exhibit line-profile variations from nonradial oscillations (δ Scuti stars, β Cephei stars, Ap stars, slowly pulsating B stars, γ Dor stars, ZZ Ceti stars, and possibly some K giants) all have associated photometric variability. Thus, a lack of photometric variations at the 0.0001 mag level in the planetary-candidate stars argues against nonradial pulsations as the cause of the radial-velocity variations. Therefore, our photometry provides strong support for true reflex motions—planets—in the stars τ Boo, 51 Peg, υ And, ρ^1 Cnc, ρ CrB, 70 Vir, and 47 UMa, but cannot yet directly support the planetary hypothesis for 16 Cyg B or Gl 411.

5.2. *Direct Detection of Planets in Reflected Light*

Charbonneau, Jha, & Noyes (1998) have modeled the combination of a spectrum of a Sun-like star with the reflected spectrum of a planet in a short-period orbit around the star. They find that for a sufficiently high albedo, the reflected spectrum from the planet may produce small but detectable distortions in the combined spectral line profiles of the star and planet. Hatzes et al. (1998) have searched for this reflected light of the planetary companion of 51 Peg in their high-resolution spectra. Their negative result implies that the planet is at least 2000 times fainter than the star, in agreement with the small semiamplitude of our photometry listed in Table 4. Here we examine the possibility that in our photometry we might similarly detect the reflected light from one of the short-period planets as the planet's illumination changes the combined light as a function of orbital phase. To estimate the amplitude of the expected phase effect, we consider that if Jupiter (with a radius of 11.2 $R_\oplus$ and an albedo of 0.70) were moved to within 0.051 AU of the Sun (51 Peg b's orbital radius) and then viewed at interstellar distances and a high orbital inclination, the differing phases of illumination would produce a light curve with an amplitude of 0.00004 mag. If its mass were reduced to the equivalent of 51 Peg b's minimum mass, the effects of insolation would swell its radius to roughly 1.4 $R_{\rm Jup}$ (Guillot et al. 1997), thus doubling its reflective surface area and photometric amplitude to about 0.00008 mag.

The precision of our photometry is approaching the precision needed to detect phase effects of this magnitude. The semiamplitudes of the photometric data and their errors listed in Table 4 come directly from least-squares sine fits to the data on the planetary orbital periods. The semiamplitudes are all 0.0001 or 0.0002 mag, and their error bars are all approximately 0.0001 mag, although half of them are a bit smaller (0.00009 mag). This is comparable to the size of the phase effect estimated above. Since the phase effect is strictly repeating, improvements to the precision of the phase curves are possible with additional observations over more cycles, even without improvement in the precision of individual observations. Concentrated observing efforts over the next couple of years may bring the precision down to around 0.00005 mag. Confirmation of an observed reflection effect could come from the phase of minimum of the observed light curve: the minimum of the phase effect must occur at phase 0.0, the time of inferior conjunction (planet in front) computed from the radial-velocity observations. This is when the dark, unlit hemisphere of the planet faces the earth. The semiamplitude results in Table 4 show that we have achieved the highest precision for τ Boo, ρ^1 Cnc, and ρ CrB. The phases of minimum of the sine fits to the photometry of these systems are 0.79 ± 0.13, 0.84 ± 0.11, and 0.15 ± 0.13, respectively, all between 1 and 2 σ of phase 0.0 (although the error bars are still rather large).

Continued monitoring of the short-period systems is needed to see whether their phase effects become unambiguously detectable. Alternatively, negative results of sufficiently high precision would provide constraints on combinations of radius, albedo, and inclination—useful for validating models of the atmospheres of short-period extrasolar planets (e.g., Seager & Sasselov 1998; Marley et al. 1999; Seager et al. 1999). The calculations of Marley et al. (1999) suggest that Strömgren b and y passbands should be near optimal for detecting the reflected light, even for hot, cloud-free planetary atmospheres that would absorb most radiation beyond 0.6 μm. Seager et al. (1999) present the results of detailed calculations of predicted optical photometric light curves of short-period planets with reflectivities determined by different particle sizes of various condensates in their atmospheres. For sufficiently large particle sizes (greater than 1 μm), they find photometric amplitudes as high as the 0.00008 mag amplitude estimated above, which may eventually be detectable by the APTs. For smaller particles, the predicted amplitudes decrease drastically, some to less than 0.000001 mag, far below any possible ground-based detection limit. Charbonneau et al. (1999) have just published the results of their spectroscopic search for the reflected light from τ Boo b and report the reflected light flux to be less than 0.00005 mag. This implies a planetary geometric albedo of 0.3 or less near 480 nm, assuming the planetary radius is $1.2R_{\rm Jup}$.

5.3. *Transit Search Results*

Our photometry shows that transits definitely do not occur in τ Boo, 51 Peg, υ And, and ρ^1 Cnc, and probably do not occur in ρ CrB and 70 Vir. Our results are inconclusive for 47 UMa, and we do not have the data to address the question for 16 Cyg B and Gl 411. However, the transit probabilities are very small for these last three systems (Table 4). Using the transit probabilities given in Table 4, computed as the ratios of the stellar radii to the semimajor axes of the planetary orbits (Schneider 1996), we calculate the probability of finding at least one transit from among the six planets that have negative transit-search results. This is given by

$$P(\text{one transit}) = 1 - P(\text{no transits}) , \quad (8)$$

where P(no transits) is the probability of finding no transits. This, in turn, is given by

$$P(\text{no transits}) = P_1(\text{no transits}) \times P_2(\text{no transits}) \times \ldots \times P_6(\text{no transit}) , \quad (9)$$

where P_i(no transits) is 1 minus the transit probability from Table 4. Then,

$$P(\text{no transits}) = 0.61 . \quad (10)$$

Therefore, our negative transit-search results are not yet problematical, since there is a greater than even chance (61%) of *not* finding a transit in this sample. However, as additional short-period, Jupiter-sized planetary candidates are found, the probability of finding a transit will increase significantly. Continued failure to find transits would begin to cast doubt on the planetary hypothesis as the most viable explanation for the radial-velocity variations. Success, on the other hand, will lead to direct measurements of extrasolar planet sizes and densities.

The predicted depths of the planetary transits in this paper are based on planetary radii computed from the models of Guillot et al. (1997). These models assume a composition of hydrogen and helium in solar proportions with no rocky core and an albedo similar to Jupiter's, and include the atmospheric enlargement effects of insolation from the host star in each system. Observed transits with depths significantly less than those predicted would imply a higher density than predicted by the models and indicate the presence of a rocky core.

The transit-search light curve of υ And in the bottom panel of Figure 5 can be used to estimate a limit to the transit depth we could observe in our photometry. We replot those data here in Figure 10 and adjust the observations that fall within the transit window downward by 0.001 mag in order to simulate a shallow transit. The dashed line across the top of the window corresponds to the out-of-transit light level and renders the drop in light easily visible. The 40 observations within the transit window have a standard deviation from their mean of 0.0010 mag; the standard deviation of their mean is 0.0002 mag. Therefore, this transit corresponds to a 5 σ event and implies that a transit of a short-period planet occurring at the predicted time of conjunction should be detectable even for depths approaching 0.0002 mag, especially because repeated observations of successive events could be combined. Since the transit of a $1R_\oplus$ planet across a 1 $R_\odot$ star would produce a transit depth of 0.000084 mag, our 0.0002 mag limit corresponds to the transit of a $1.5R_\oplus$ planet across a 1 $R_\odot$ star. If the short–orbital-period planets under consideration in this paper are not gas giants, as currently assumed, but have rocky compositions throughout, their radii would be only $\sim\frac{1}{3}R_{\rm Jup}$ (Guillot et al. 1996). Therefore, they would give transit depths of only 0.001 mag or so, but they would still be detectable in our photometry.

5.4. *Year-to-Year Stellar Photometric Variations*

Our measure of year-to-year photometric variations is the standard deviation of a star's yearly mean magnitudes

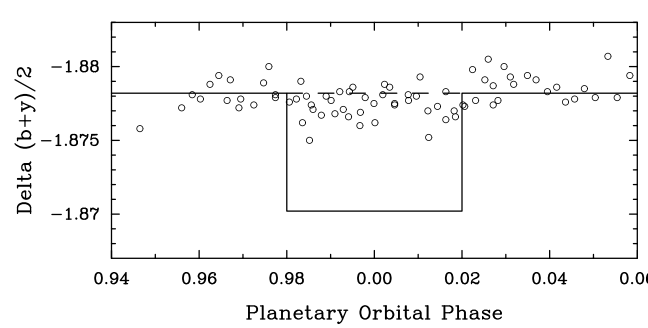

FIG. 10.—Transit-search light curve of υ And from the bottom panel of Fig. 5, replotted here with the observations that fall within the transit window, adjusted downward by 0.001 mag to simulate a shallow transit. The dashed line across the top of the transit window corresponds to the out-of-transit light level and renders the drop in light easily visible. This demonstrates that transits of the short-period planets sought in this paper would have been detectable even for planets with rocky compositions.

(from Table 3) with respect to the mean of the yearly means. These standard deviations are given as $\sigma_{\rm long}$ in column (3) of Table 4. We find significant long-term variations only in τ Boo, with $\sigma_{\rm long} = 0.0008$ mag. As discussed in the τ Boo section above, these variations are intrinsic to τ Boo and are not the result of measurement errors or variations in the comparison stars. All the other stars have $\sigma_{\rm long}$ less than 0.0001 or 0.0002 mag, about the limit of our measurement precision, or have comparison stars that we suspect are slightly variable from year to year.

τ Boo has the shortest observed rotation period and is the youngest star in this sample. The range in its yearly mean magnitudes is $\sim$0.002 mag, roughly twice the 0.0008 mag long-term variation in the Sun's total irradiance observed with the ACRIM radiometer on board the *SMM* satellite (Willson 1997). Although τ Boo, an F7 dwarf, has a more shallow convection zone than the Sun, its much shorter rotation period still means that enough magnetic activity is generated through the dynamo mechanism for it to produce long-term brightness variations exceeding the Sun's irradiance variations associated with the sunspot cycle.

5.5. Ca II *H and K Variability*

In Papers I and II, we noted that aside from τ Boo, which shows a large-amplitude Doppler velocity variation, the stars then announced to have planetary companions were relatively inactive, with little or no surface magnetic activity, i.e., Ca II flux variability. Low activity is a bias favoring the detection of low-amplitude Doppler reflex velocities, especially if orbital periods are suspected near timescales of activity variability, e.g., rotational modulation. Five of the nine stars here show little variability, supporting planets instead of surface activity variations as the cause of Doppler variations. Long-term variability is clearly evident for Gl 411, ρ^1 Cnc, and υ And, as well as τ Boo. For stars whose reported planetary orbital periods differ from the observed activity periods, or whose reflex velocity amplitude is substantial, activity variations do not refute the planet hypothesis. For stars whose reported planets have orbital periods of years, such as υ And (Butler et al. 1999) and ρ^1 Cnc (Marcy & Butler 1998), the effect of long-term surface activity variations on radial-velocity variations must be assessed.

Many thanks go to Lou Boyd and Don Epand for their efforts to develop and operate Fairborn Observatory. G. W. H. acknowledges helpful discussions with Didier Saumon, Robert Noyes, and Robert Jastrow. We thank Geoff Marcy and Robert Noyes for providing us with updated orbital ephemerides to aid in our search for photometric transits. Astronomy with automated telescopes at Tennessee State University has been supported by the National Aeronautics and Space Administration, most recently through NASA grants NCC 2-977, NCC 5-96, and NCC 5-228 (which funds TSU's Center for Automated Space Science), the National Science Foundation, most recently through NSF grants HRD-9550561 and HRD-9706268 (which funds TSU's Center for Systems Science Research), and the Richard Lounsbery Foundation.

We are indebted to past and present colleagues of the HK Project and Mount Wilson Observatory, without whom the 33 yr Ca II H and K database would not exist. V. Cristina Cristian assisted with the calibration of the HK data used in this paper. Research for the HK Project has been supported by the Richard Lounsbery Foundation, the Scholarly Studies Program and the James Arthur Funds of the Smithsonian Institution, The Olin Wilson Fund of the Mount Wilson Institute, MIT Space Grants 5700000633 and 7A06, NASA grant NAG 5-7635, and several generous individuals.

REFERENCES

Baliunas, S. L., Donahue, R. A., Soon, W., & Henry, G. W. 1998, in ASP Conf. Ser. 154, The 10th Cambridge Workshop on Cool Stars, Stellar Systems, and the Sun, ed. R. A. Donahue & J. A. Bookbinder (San Francisco: ASP), 153

Baliunas, S. L., Henry, G. W., Donahue, R. A., Fekel, F. C., & Soon, W. H. 1997, ApJ, 474, L119 (Paper II)

Baliunas, S. L., & Jastrow, R. 1990, Nature, 348, 520

Baliunas, S. L., et al. 1985, ApJ, 294, 310

———. 1995, ApJ, 438, 269

Berriman, G., Reid, N., & Leggett, S. K. 1992, ApJ, 392, L31

Blackwell, D. E., & Lynas-Gray, A. E. 1994, A&A, 282, 899

Boss, A. P. 1997, Science, 276, 1836

———. 1998, ApJ, 503, 923

Brown, T. M., et al. 1998, ApJ, 494, L85

Butler, R. P., & Marcy, G. W. 1996, ApJ, 464, L153

Butler, R. P., Marcy, G. W., Fischer, D. A., Brown, T. W., Contos, A. R., Korzennik, S. G., Nisenson, P., & Noyes, R. W. 1999, ApJ, 526, 916

Butler, R. P., Marcy, G. W., Vogt, S. S., & Apps, K. 1998, PASP, 110, 1389

Butler, R. P., Marcy, G. W., Williams, E., Hauser, H., & Shirts, P. 1997, ApJ, 474, L115

Charbonneau, D., Jha, S., & Noyes, R. W. 1998, ApJ, 507, L153

Charbonneau, D., et al. 1999, ApJ, 522, L145

Cochran, W. D., Hatzes, A. P., Butler, R. P., & Marcy, G. W. 1997, ApJ, 483, 457

Dominik, C., Laureijs, R. J., Jourdain de Muizon, M., & Habing, H. J. 1998, A&A, 329, L53

Donahue, R. A. 1993, PhD Thesis, New Mexico State Univ.

———. 1998, in ASP Conf. Ser. 154, The Tenth Cambridge Workshop on Cool Stars, Stellar Systems, and the Sun, ed. R. A. Donahue & J. A. Bookbinder (San Francisco: ASP), CD-834

Donahue, R. A., Baliunas, S. L., Frazer, J., French, H., & Lanning, H. 1986, in The Fourth Cambridge Workshop on Cool Stars, Stellar Systems, and the Sun, ed. M. Zeilik & D. M. Gibson (New York: Springer), 281

Eaton, J. A., Boyd, L. J., & Henry, G. W. 1996, BAAS, 28, 841

Edvardsson, B., Andersen, J., Gustafsson, B., Lambert, D. L., Nissen, P. E., & Tomkin, J. 1993, A&A, 275, 101

Eggen, O. J. 1979, ApJ, 230, 786

Fekel, F. C. 1997, PASP, 109, 514

Fekel, F. C., & Henry, G. W. 1998, in ASP Conf. Ser. 154, The 10th Cambridge Workshop on Cool Stars, Stellar Systems, and the Sun, ed. R. A. Donahue & J. A. Bookbinder (San Francisco: ASP), CD-755

Fischer, D. A., Marcy, G. W., Butler, R. P., Vogt, S. S., & Apps, K. 1999, PASP, 111, 50

Flower, P. J. 1996, ApJ, 469, 355

Ford, E. B., Rasio, F. A., & Sills, A. 1998, ApJ, 514, 411

Friel, E., Cayrel de Strobel, G., Chmeilewski, Y., Spite, M., Lèbre, A., & Bentolila, C. 1993, A&A, 274, 825

Fuhrmann, K., Pfeiffer, M. J., & Bernkopf, J. 1997, A&A, 326, 1081

———. 1998, A&A, 336, 942

Gatewood, G. 1996, BAAS, 28, 885

Gatewood, G., et al. 1992, AJ, 104, 1237

Giampapa, M. S., et al. 1996, ApJ, 463, 707

Gonzalez, G. 1997, MNRAS, 285, 403

———. 1998, A&A, 334, 221

Gonzalez, G., & Vanture, A. D. 1998, A&A, 339, L29

Gray, D. F. 1986, PASP, 98, 319

———. 1997, Nature, 385, 795

———. 1998, Nature, 391, 153

Gray, D. F., & Hatzes, A. P. 1997, ApJ, 490, 412

Guillot, T., et al. 1996, ApJ, 459, L35

———. 1997, in Astronomical and Biochemical Origins and the Search for Life in the Universe, ed. C. B. Cosmovici, S. Bowyer, & D. Werthimer (Balogna: Editrice Compositori), 343

Hall, J. C., ed. 1998, Solar Analogs: Characteristics and Optimum Candidates (Flagstaff: Lowell Obs.)

Hatzes, A. P. 1996, PASP, 108, 839

Hatzes, A. P., & Cochran, W. D. 1998, ApJ, 502, 944

Hatzes, A. P., Cochran, W. D., & Bakker, E. J. 1998, ApJ, 508, 380

Henry, G. W. 1995a, in ASP Conf. Ser. 79, Robotic Telescopes: Current Capabilities, Present Developments, and Future Prospects for Automated Astronomy, ed. G. W. Henry & J. A. Eaton (San Francisco: ASP), 37

———. 1995b, in ASP Conf. Ser. 79, Robotic Telescopes: Current Capabilities, Present Developments, and Future Prospects for Automated Astronomy, ed. G. W. Henry & J. A. Eaton (San Francisco: ASP), 44

Henry, G. W. 1999, PASP, 111, 845
Henry, G. W., Baliunas, S. L., Donahue, R. A., Soon, W. H., & Saar, S. H. 1997a, ApJ, 474, 503 (Paper I)
Henry, T. J., Ianna, P. A., Kirkpatrick, J. D., & Jahreiss, H. 1997b, AJ, 114, 388
Henry, T. J., Kirkpatrick, J. D., & Simons, D. A. 1994, AJ, 108, 1437
Henry, T. J., & McCarthy, D. W. 1990, ApJ, 350, 334
Hershey, J. L., & Lippincott, S. L. 1982, AJ, 87, 840
Horne, J. H., & Baliunas, S. L. 1986, ApJ, 302, 757
Lippincott, S. L. 1960, AJ, 65, 445
Lockwood, G. W., Skiff, B. A., & Radick, R. R. 1997, ApJ, 485, 789
Marcy, G. W., & Benitz, K. J. 1989, ApJ, 344, 441
Marcy, G. W., & Butler, R. P. 1996, ApJ, 464, L147
———. 1998, ARA&A, 36, 57
Marcy, G. W., et al. 1997, ApJ, 481, 926
Marley, M. S., et al. 1999, ApJ, 513, 879
Mayor, M., & Queloz, D. 1995, Nature, 378, 355
———. 1996, in ASP Conf. Ser. 109, Cool Stars, Stellar Systems, and the Sun, ed. R. Pallavicini & A. K. Dupree (San Francisco: ASP), 35
Mayor, M., Queloz, D., Beuzit, J.-L., Mariott, J.-M., Naef, D., Perrier, C., & Sivan, J.-P. 1998, in Protostars & Planets IV, ed. V. Manings, in press
Mermilliod, J.-C., & Mermilliod, M. M. 1994, Catalogue of Mean UBV Data on Stars (New York: Springer)
Mould, J. R. 1978, ApJ, 226, 923
Ng, Y. K., & Bertelli, G. 1998, A&A, 329, 943
Noyes, R. W., Hartmann, L. W., Baliunas, S. L., Duncan, D. K., & Vaughan, A. H. 1984, ApJ, 279, 763
Noyes, R. W., et al. 1997a, ApJ, 483, L111
———. 1997b, ApJ, 487, L195
O'Neal, D., & Neff, J. E. 1997, AJ, 113, 1129
Perrin, M. N., Hejlesen, P. M., Cayrel del Strobel, G., & Cayrel, R. 1977, A&A, 54, 779
Perryman, M. A. C., et al. 1997, The Hipparcos and Tycho Catalogues (Noordwijk: ESA)
Queloz, D., et al. 1999, ApJ, in preparation
Saar, S. H., Butler, R. P., & Marcy, G. W. 1998, ApJ, 498, L153
Saar, S. H., & Donahue, R. A. 1997, ApJ, 485, 319
Sandquist, E., et al. 1998, ApJ, 506, L65
Saumon, D., Hubbard, W. B., Burrows, A., Guillot, T., Lunine, J. I., & Chabrier, G. 1996, ApJ, 460, 993
Schneider, J. 1996, A&A, 241, 35
Seager, S., & Sasselov, D. D. 1998, ApJ, 502, L157
Seager, S., Whitney, B., & Sasselov, D. D. 1999, ApJ, submitted
Soderblom, D. R., Duncan, D. K., & Johnson, D. R. H. 1991, ApJ, 375, 722
Trilling, D. E., & Brown, R. H. 1998, Nature, 395, 775
Trilling, D. E., et al. 1998, ApJ, 500, 428
Ward, W. R. 1997, ApJ, 482, L211
Weis, E. W. 1994, AJ, 107, 1135
Willson, R. C. 1997, Science, 277, 1963
Wilson, O. C. 1978, ApJ, 226, 379